

Original Article

A functional autophagy pathway is essential for BMP9-induced osteogenic differentiation of mesenchymal stem cells (MSCs)

Xia Zhao^{1,2}, Bo Huang^{2,3}, Hao Wang^{2,4}, Na Ni^{2,4}, Fang He^{2,5}, Qing Liu^{2,6}, Deyao Shi^{2,7}, Connie Chen², Piao Zhao^{2,5}, Xi Wang^{2,4}, William Wagstaff², Mikhail Pakvasa², Andrew Blake Tucker², Michael J Lee², Jennifer Moriatis Wolf², Russell R Reid^{2,8}, Kelly Hynes², Jason Strelzow², Sherwin H Ho², Tengbo Yu¹, Jian Yang⁹, Le Shen^{2,10}, Tong-Chuan He^{2,10}, Yongtao Zhang^{1,2}

¹Department of Orthopaedic Surgery, The Affiliated Hospital of Qingdao University, Qingdao 266061, China; ²Molecular Oncology Laboratory, Department of Orthopaedic Surgery and Rehabilitation Medicine, The University of Chicago Medical Center, Chicago, IL 60637, USA; ³Department of Clinical Laboratory Medicine, The Second Affiliated Hospital of Nanchang University, Nanchang 330031, China; ⁴Ministry of Education Key Laboratory of Diagnostic Medicine, and School of Laboratory and Diagnostic Medicine, Chongqing Medical University, Chongqing 400016, China; ⁵Departments of Medicine/Gastroenterology, Orthopaedic Surgery, The First Affiliated Hospital of Chongqing Medical University, Chongqing 400016, China; ⁶Departments of Orthopaedic Surgery and Spine Surgery, Second Xiangya Hospital, Central South University, Changsha, China; ⁷Department of Orthopaedics, Union Hospital of Tongji Medical College, Huazhong University of Science and Technology, Wuhan, China; ⁸Section of Plastic Surgery and Laboratory of Craniofacial Biology and Development, and Section of Surgical Research, Department of Surgery, The University of Chicago Medical Center, Chicago, IL 60637, USA; ⁹Department of Biomedical Engineering, Materials Research Institute, The Huck Institutes of The Life Sciences, The Pennsylvania State University, University Park, PA 16802, USA; ¹⁰Section of Surgical Research, Department of Surgery, The University of Chicago Medical Center, Chicago, IL 60637, USA

Received February 21, 2021; Accepted March 15, 2021; Epub May 15, 2021; Published May 30, 2021

Abstract: Mesenchymal stem cells (MSCs) are capable of differentiating into bone, cartilage and adipose tissues. We identified BMP9 as the most potent osteoinductive BMP although detailed mechanism underlying BMP9-regulated osteogenesis of MSCs is indeterminate. Emerging evidence indicates that autophagy plays a critical role in regulating bone homeostasis. We investigated the possible role of autophagy in osteogenic differentiation induced by BMP9. We showed that BMP9 upregulated the expression of multiple autophagy-related genes in MSCs. Autophagy inhibitor chloroquine (CQ) inhibited the osteogenic activity induced by BMP9 in MSCs. While overexpression of ATG5 or ATG7 did not enhance osteogenic activity induced by BMP9, silencing *Atg5* expression in MSCs effectively diminished BMP9 osteogenic signaling activity and blocked the expression of the osteogenic regulator Runx2 and the late marker osteopontin induced by BMP9. Stem cell implantation study revealed that silencing *Atg5* in MSCs profoundly inhibited ectopic bone regeneration and bone matrix mineralization induced by BMP9. Collectively, our results strongly suggest a functional autophagy pathway may play an essential role in regulating osteogenic differentiation induced by BMP9 in MSCs. Thus, restoration of dysregulated autophagic activity in MSCs may be exploited to treat fracture healing, bone defects or osteoporosis.

Keywords: BMP9, autophagy, mesenchymal stem cells, lineage-specific differentiation, osteogenic signaling, bone formation

Introduction

Mesenchymal stem cells (MSCs) are multipotent progenitors, and they can differentiate into several types of tissues such as bone, cartilage, adipose, and muscle [1-6]. While the exact

mechanisms are not fully understood, osteogenic lineage-specific differentiation of MSCs is tightly modulated by multiple major signaling pathways, such as TGF- β /BMP superfamily members, WNT/ β -catenin, NOTCH ligands and receptors, and FGFs to name a few [3, 7-18].

Autophagy participates in BMP9-induced osteogenesis

Among those osteogenic regulators, BMPs represent a group of the most potent osteogenic factors [19-21].

BMPs are members of TGF- β superfamily [3, 19, 20, 22], and the 14 types of BMPs exist in humans and rodents [19, 20, 23, 24]. We carried out a systematic study, analyzed the osteogenic capability of the 14 human BMPs, and identified the least known BMP9 as the strongest osteogenic BMP in MSCs [19, 21, 25-28]. BMP9, unlike BMP2 and BMP7, is refractory to the inhibitory effect exerted by the potent antagonist noggin [29]. We also showed that TGF- β /BMP-1R ALK1 and ALK2 are critical for transmitting BMP9 osteogenic signaling [30] and subsequently regulating downstream target genes in MSCs [31-38]. We further demonstrated that noncoding RNAs may play an important role in BMP9-initiated osteogenic signaling [39-41], while we and others revealed that BMP9 can cross-talk with many pathways in regulating osteogenic differentiation [16, 35-37, 42-49]. But, the detailed mechanisms underlying BMP9-induced osteogenesis remain indeterminate.

Emerging evidence indicates that autophagy may play an important role in bone homeostasis [50-52]. As an evolutionarily conserved cytoplasmic membrane-trafficking pathway for shuttling organelles and/or proteins to lysosomes for degradation and recycling, autophagy is considered one of the primary catabolic pathways, in which cells are digested to recover nutrients and energy [50, 53-55]. Autophagy is indispensable for cell homeostasis and stress responses [52]. Multiple proteins involved in autophagy activities, such as autophagy-related (ATG) proteins, are critical to the survival and differentiation of osteoblasts, osteocytes, and osteoclasts [50-52]. As the paradoxical functions of autophagy in maintaining cell homeostasis and stress responses demand a delicate and fine-tuned regulation of autophagic activity, dysregulated autophagic activity may disturb the balance between bone formation and bone resorption, leading to the development and/or progression of bone disorders, such as osteoporosis and Paget's disease [50-52, 55]. Nonetheless, since autophagy is known to play paradoxical roles in many cellular processes, the exact mechanisms underlying autophagy-regulated bone homeostasis remain to be thoroughly elucidated.

In this study, we studied whether or not the autophagy pathway played any role in osteogenic differentiation induced by BMP9 in MSCs. We showed that BMP9 effectively upregulated the expression of multiple autophagy-related genes (ATGs) in MSCs. Autophagy inhibitor chloroquine (CQ) was shown to significantly inhibit the osteogenic activity induced by BMP9 in MSCs. While an overexpression of ATG5 or ATG7 did not enhance BMP9-induced osteogenic activity, silencing *Atg5* in MSCs effectively diminished BMP9 osteogenic signaling activity and blocked the expression of the osteogenic regulator Runx2 and the late marker osteopontin induced by BMP9. *In vivo* stem cell implantation experiments revealed that silencing *Atg5* in MSCs profoundly inhibited ectopic bone formation and bone matrix mineralization induced by BMP9. Collectively, these findings suggest that effective osteogenesis induced by BMP9 may require functional autophagy pathway in MSCs. Therefore, restoration of dysregulated autophagic activity in MSCs may be explored to treat bone fracture healing, bone defects, or osteoporosis.

Material and methods

Chemicals, cell culture and medium

Mouse imBMSCs are reversibly immortalized mouse bone marrow stromal cells previously characterized [56]. HEK-293 cells were obtained from ATCC, while 293pTP and RAPA cells were derived from HEK-293 cells as described [57, 58]. The above cell lines were cultured in DMEM containing 10% FBS, containing penicillin (100 U/ml) and streptomycin (100 μ g/ml) at 37°C in 5% CO₂ as described [59-63]. All other chemicals were purchased from Sigma-Aldrich or Thermo Fisher Scientific.

Generation and amplification of adenoviral vectors Ad-BMP9, Ad-ATG5, Ad-ATG7, AdR-simAtg5 and Ad-GFP

We constructed recombinant adenoviruses using the AdEasy system [64-66]. Specifically, the human BMP9, human ATG5, and human ATG7 coding regions were amplified by Hi-Fi PCR, cloned into an adenoviral shuttle vector to produce recombinant adenovirus plasmids and subsequently adenoviruses in packaging cell lines such as 293pTP and RAPA cells [57, 58], yielding Ad-BMP9, Ad-ATG5 and Ad-ATG7, all of

Autophagy participates in BMP9-induced osteogenesis

which also co-express GFP as a tracking marker.

For the construction of silencing *Atg5* adenoviral vector, three siRNAs silencing the coding region of mouse *Atg5* were designed by using Invitrogen's BLOCK-IT RNAi Designer program, simultaneously assembled into our recently-developed FAMSi vector system [67], which was optimized on the basis of our previously-established siRNA expression systems [68-71], and subsequently subcloned into our homemade adenoviral vector as described [17, 37, 72, 73]. Recombinant adenovirus AdR-simAtg5 was generated in 293pTP or RAPA cells. The AdR-simAtg5 co-expresses RFP as a tracking marker. Ad-GFP was used as a control virus as described [70, 74-77]. Polybrene (5 µg/ml) was included in all adenoviral infections to enhance adenoviral infection efficiency as described [78].

RNA purification & touchdown quantitative PCR (TqPCR)

Total RNA was extracted with TRIZOL Reagent and used for reverse transcription reactions using random 6 mers and M-MuLV RT (New England Biolabs, Ipswich, MA). RT products were used as TqPCR templates. TqPCR primers were designed by using Primer3 Plus program (Supplementary Table 1). TqPCR analysis was performed as described [24, 45, 79-82]. Briefly, SYBR Green (Bimake, Houston, TX) qPCR was set up with the following cycling parameters: 95°C × 3' for 1 cycle; 95°C × 20", 66°C × 10" per cycle, then -3°C each cycle for 4 cycles; followed by 95°C × 10", 55°C × 15", and 70°C × 1' for 40 cycles. All reactions were normalized with the expression level of reference gene *Gapdh*. The $2^{-\Delta\Delta Ct}$ method was used to determine relative gene expression.

Determination of alkaline phosphatase (ALP) activity

Different adenoviruses were used to infect subconfluent imBMSCs. At the indicated time points (usually 2, 4, 6 days after infection), the Great Escape SEAP Chemiluminescence Assay was used to quantitatively assess ALP activities as previously described [37, 83-85]. Each assay condition was conducted in triplicate.

Qualitative ALP activity was assessed with histochemical staining 4 days and 6 days after

infection. Briefly, the imBMSCs were fixed with glutaraldehyde, and stained with a mixture of naphthol AS-MX phosphate and Fast Blue BB salt as described [25, 26, 33, 86, 87]. The stains were washed with PBS and recorded. Each staining condition was conducted in triplicate.

Alizarin Red S stain

Subconfluent imBMSCs were plated in 24-well culture plates, infected with appropriate adenoviral vectors, and cultured in complete DMEM with ascorbic acid (50 µg/ml) and β-glycerophosphate (10 mM). At the endpoints of assays, the cells were fixed and stained with Alizarin Red S to visualize mineral nodules as previously reported [25, 88, 89]. The stained calcium mineral nodules were recorded. Alizarin Red S stains were quantified by dissolving in 10% acetic acid and measuring absorbance at 405 nm. Each staining assay condition was conducted in triplicate.

Ectopic bone formation

The use and care of animals was approved by the Institutional Animal Care and Use Committee. Subcutaneous injection procedure was conducted as described [83, 88, 90-96]. Experimentally, subconfluent imBMSCs were co-infected with appropriate combinations of adenoviruses for 36 h, harvested, resuspended in sterile PBS/PPCN scaffold material mix (~5 × 10⁶ cells in 50 µl/injection), and subcutaneously injected into the flanks of nude mice (Envigo; n=4/group, female, 6-wk-old). At 5 wk after injection, the animals were euthanized for harvesting the bony masses.

MicroCT (µCT) imaging and data analysis

Retrieved bony masses were fixed in 10% PBS-buffered formalin and imaged by using the µCT component of the GE triumph trimodality imaging system. The acquired imaging data were analyzed using Amira 6.0 (Visage Imaging, Inc.) as previously described [35, 49, 97, 98].

Histologic evaluation and Masson's trichrome staining

The above fixed masses were subjected to decalcification and paraffin embedding. 5 µm sections were used for H&E histologic evaluation and Masson's trichrome staining as previously reported [96, 99-103].

Autophagy participates in BMP9-induced osteogenesis

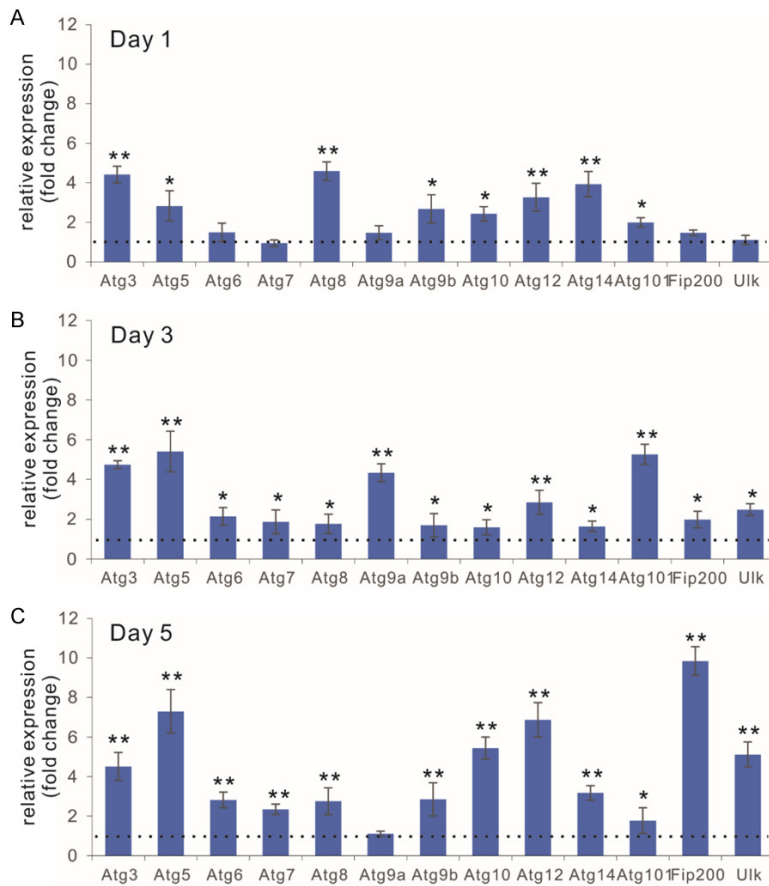


Figure 1. BMP9 upregulates the expression of multiple autophagy genes in MSCs. Subconfluent MSCs were infected with Ad-BMP9 or Ad-GFP. Total RNA was isolated at 1 day (A), 3 days (B) and 5 days (C) after infection, and subjected to RT-qPCR analysis of the expression of major regulators of the autophagy pathway. Relative expression was calculated as fold changes over Ad-GFP infected cells (dotted lines). “*” P<0.05, “**” P<0.01, compared with that of the Ad-GFP group for respective genes.

Statistical analysis

We performed all quantitative studies in triplicate. The statistical comparison of the means between two groups was determined by Student’s t test. The P<0.05 was cutoff for statistical significance.

Results

BMP9 can upregulate the expression of multiple autophagy genes in MSCs

To determine whether or not autophagy plays any role in osteogenic differentiation induced by BMP9 in MSCs, we first analyzed if BMP9 would affect the expression of 13 of the important genes in the autophagy pathway. When subconfluent imBMSCs were transduced with

Ad-BMP9 or Ad-GFP control adenovirus, eight of the tested 13 genes were up-regulated by BMP9 at 24 h post infection (**Figure 1A**), while BMP9 up-regulated all 13 genes at 72 h after infection (**Figure 1B**). Even at 5 days after infection, BMP9 up-regulated the expression of 12 of the 13 tested genes in the autophagy pathway (**Figure 1C**). Similar results were obtained in other types of MSCs stimulated with BMP9 (data not shown). Our results demonstrate that BMP9 can up-regulate multiple autophagy genes in MSCs, especially *Atg3*, *Atg5*, *Atg8*, *Atg9a*, *Atg10*, *Atg14*, *Atg101*, *Fip200*, and *Ulk*, suggesting that autophagy may play an important role in osteogenic differentiation induced by BMP9 in MSCs.

Autophagy blockade effectively inhibits ALP activity and matrix mineralization induced by BMP9 in MSCs

We next tested the effect of autophagy inhibition on osteogenic differentiation stimulated by BMP9 in MSCs.

Even though chloroquine (CQ) has been widely used as an autophagy inhibitor in cancer cells, it was not well established what the optimal non-lethal concentrations of CQ are for MSCs. When imBMSCs were treated with a broad range of CQ (0 to 80 μ M), we found that 40 μ M CQ caused drastic cytotoxicity and cell death, while imBMSC cells were apparently healthy when CQ concentration was lower than 20 μ M (**Supplementary Figure 1A**). Furthermore, no significant cytotoxicity was observed in the imBMSC cells that were infected with Ad-BMP9 or Ad-GFP, and/or treated with up to 10 μ M CQ (**Supplementary Figure 1Ba, 1Bb**). Thus, we chose the maximal concentration of 10 μ M CQ in our experiments.

When imBMSCs were infected with Ad-BMP9 or Ad-GFP, and treated with different concentra-

Autophagy participates in BMP9-induced osteogenesis

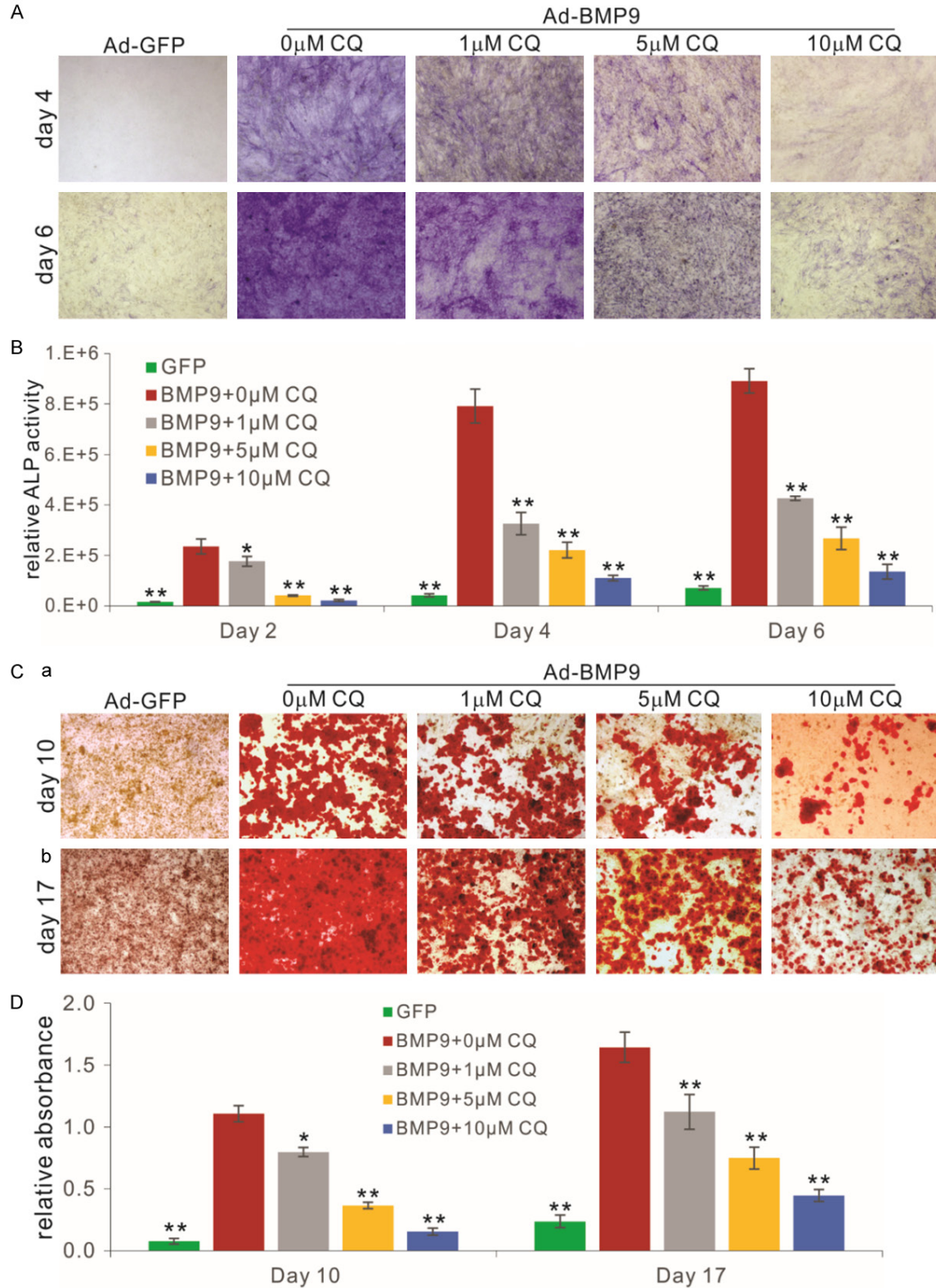


Figure 2. Autophagy blockade leads to the inhibition of BMP9-induced ALP activity and matrix mineralization in MSCs. (A, B) Autophagy inhibitor chloroquine (CQ) suppresses BMP9-induced ALP activity. Subconfluent MSCs were infected with Ad-BMP9 or Ad-GFP, and treated with the indicated concentrations of CQ. At 4 days and 6 days after infection, ALP activity was stained histochemically and representative results are shown (A). Quantitative ALP assay

Autophagy participates in BMP9-induced osteogenesis

was also carried out at 2, 4, and 6 days after infection (B). “*” $P < 0.05$, “***” $P < 0.01$, compared with that of the “Ad-BMP9+0 μM CQ” group. (C, D) Autophagy inhibitor chloroquine (CQ) diminishes BMP9-induced matrix mineralization. Subconfluent MSCs were infected with Ad-BMP9 or Ad-GFP, and treated with the indicated concentrations of CQ. At 10 days and 17 days after infection, the cells were fixed and stained with Alizarin Red staining, and representative results are shown (C). The Alizarin Red stains were dissolved and quantitatively measured (D). “*” $P < 0.05$, “***” $P < 0.01$, compared with that of the “Ad-BMP9+0 μM CQ” group.

tions of CQ, we found that ALP activity induced by BMP9 was inhibited in a dose-dependent manner at both day 4 and day 6, respectively (**Figure 2A**). Quantitative ALP activity analysis also confirmed that ALP activity stimulated by BMP9 was significantly suppressed by CQ at 2, 4, and 6 days after infection in a dose-dependent fashion (**Figure 2A**). Alizarin Red S staining assay indicates that matrix mineralization induced by BMP9 was effectively inhibited by CQ in a dose-dependent fashion at both day 10 and day 17, respectively (**Figure 2Ca, 2Cb**), which was further confirmed by the quantitative measurements of the stained mineral nodules (**Figure 2D**). Collectively, these findings suggest autophagy blockade may significantly diminish BMP9-induced osteogenesis of MSCs.

Silencing Atg5 expression effectively blunts the ALP activity and matrix mineralization induced by BMP9 in MSCs

We further analyzed the effect of overexpression or silencing of autophagy genes (e.g., *Atg5* and *Atg7*) on osteogenic differentiation induced by BMP9 in MSCs. In order to effectively overexpress autophagy genes, we engineered recombinant adenoviral vectors Ad-ATG5 and Ad-ATG7, both of which were shown to effectively transduce imBMSC cells, and could be used to co-infect imBMSC cells with Ad-BMP9 (**Supplementary Figure 2A, 2B**). For silencing *Atg5* expression in imBMSCs, we also constructed AdR-simAtg5 adenoviral vector, and showed the imBMSC cells were readily transduced by AdR-simAtg5 alone, or with Ad-BMP9 (**Supplementary Figure 2C**). We further demonstrated that *Atg5* expression in imBMSC cells was effectively silenced by AdR-simAtg5 adenoviral vector (**Supplementary Figure 2D**).

When imBMSCs were co-infected with Ad-BMP9 and Ad-ATG5, we found that ALP activity stimulated by BMP9 was not significantly enhanced by ATG5 overexpression at the tested time points (**Figure 3Aa, 3Ab**). Similarly, overexpression of ATG7 in imBMSC cells did not significantly impact BMP9-stimulated ALP activity (**Figure 3Ba, 3Bb**). We further investigated the

effect of ATG5 overexpression on late stage of osteogenesis induced by BMP9 and found that exogenous expression of ATG5 in imBMSCs did not significantly enhance matrix mineralization induced by BMP9 as determined by Alizarin Red S staining (**Figure 3Ca, 3Cb**). Similar results were obtained in the imBMSC cells co-infected with Ad-ATG7 and Ad-BMP9, and no increase in Alizarin Red S staining was observed (**Figure 3Da, 3Db**). These results indicate that exogenous expression of autophagy genes seemingly does not affect osteogenic differentiation induced by BMP9 in MSCs.

However, silencing *Atg5* in imBMSC cells effectively diminished ALP activity induced by BMP9 at 4 days and 6 days after infection (**Figure 4Aa, 4Ab**). Quantitative analysis confirmed that ALP activity stimulated by BMP9 was inhibited in the AdR-simAtg5 infected cells at 2, 4, and 6 days after infection (**Figure 4B**). Accordingly, silencing *Atg5* led to a marked decrease in Alizarin Red S staining induced by BMP9 at 10 days and 17 days after infection (**Figure 4Ca, 4Cb**), which was readily supported by the quantitative analysis of the stained mineral nodules (**Figure 4Cc**). Collectively, these findings suggest that a functional autophagy pathway may be critical to osteogenic differentiation induced by BMP9 in MSCs, consistent with the inhibitory effect exerted by CQ blockade as shown in **Figure 2**.

To elucidate potential mechanism underlying the effect of overexpressing or silencing autophagy genes in MSCs, we co-infected imBMSCs with Ad-BMP9 and/or Ad-ATG5, Ad-ATG7, or AdR-simAtg5 for 3 days, and analyzed the expression of the master osteogenic regulator Runx2 and the late osteogenic marker osteopontin (*Opn*) by qPCR. We found that overexpression of ATG5 or ATG7 did not significantly affect expression of Runx2 and *Opn* up-regulated by BMP9 (**Figure 5A, 5B**). However, silencing *Atg5* in imBMSC cells significantly diminished the expression of *Runx2* and *Opn* induced by BMP9 (**Figure 5C**). Taken together, the above findings are consistent with the hypothesis that functional autophagy pathway plays an impor-

Autophagy participates in BMP9-induced osteogenesis

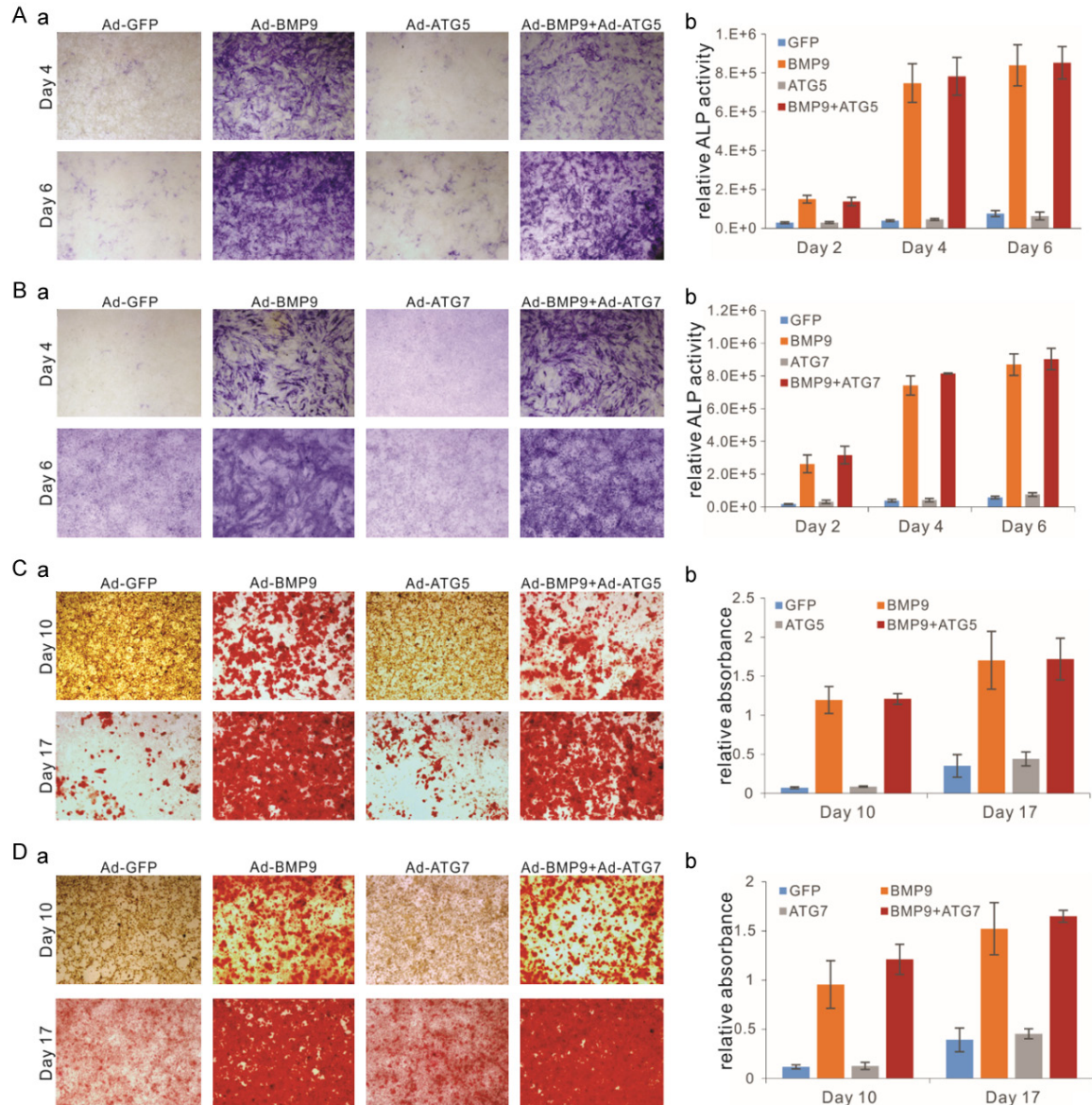


Figure 3. Exogenous expression of ATG5 or ATG7 does not affect BMP9-induced osteogenic differentiation in MSCs. (A, B) Exogenous expression of ATG5 or ATG7 does not affect BMP9-induced ALP activity. Subconfluent MSCs were infected with Ad-GFP, Ad-BMP9, and/or Ad-ATG5 (A), and/or Ad-ATG7 (B). ALP activity was qualitatively assessed with histochemical staining at 4 and 6 days after infection (a), or was quantitatively determined at 2, 4, and 6 days after infection (b). Representative results are shown. (C, D) Exogenous expression of ATG5 or ATG7 does not affect BMP9-induced matrix mineralization. Subconfluent MSCs were infected with Ad-GFP, Ad-BMP9, and/or Ad-ATG5 (C), and/or Ad-ATG7 (D). Alizarin Red staining was carried out at 10 and 17 days after infection (a), followed by dissolving the stains for quantitative absorbance measurement (b). Representative results are shown.

tant role in osteogenic differentiation initiated by BMP9 in MSCs.

Silencing Atg5 inhibits ectopic bone formation induced by BMP9 in MSCs

Lastly, we examined the effect of overexpressing or silencing autophagy genes on *in vivo*

bone formation induced by BMP9. When imBMSCs were co-infected with combinations of Ad-GFP or Ad-BMP9, with Ad-ATG5, Ad-ATG7, or AdR-simAtg5, and implanted into the flanks of nude mice for 5 weeks. No retrievable masses were found in the Ad-GFP control, Ad-ATG5 only, Ad-ATG7 only, and AdR-simAtg5 only groups. Apparent masses were readily retrieved from

Autophagy participates in BMP9-induced osteogenesis

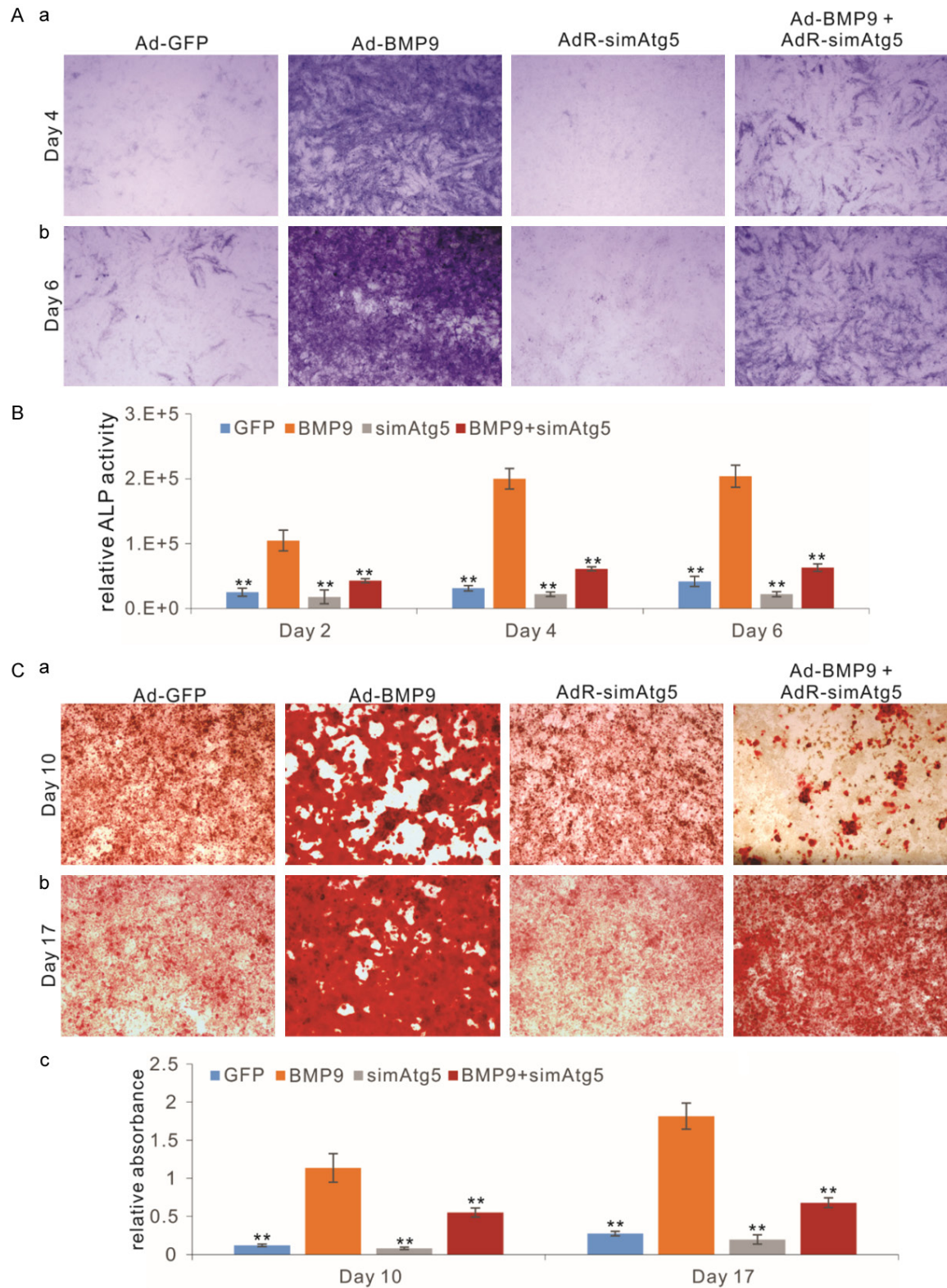


Figure 4. Silencing ATG5 significantly diminishes BMP9-induced ALP activity and matrix mineralization in MSCs. (A, B) Silencing Atg5 inhibits BMP9-induced ALP activity. Subconfluent MSCs were infected with Ad-GFP, Ad-BMP9, and/or AdR-simAtg5. ALP activity was qualitatively assessed with histochemical staining at 4 days (a) and 6 days (b) after infection, or was quantitatively determined at 2, 4, and 6 days after infection (B). Representative results are shown. “**” $P < 0.01$, compared with that of the Ad-BMP9 group. (C) Silencing Atg5 inhibits BMP9-induced matrix mineral-

Autophagy participates in BMP9-induced osteogenesis

ization. Subconfluent MSCs were infected with Ad-GFP, Ad-BMP9, and/or AdR-simAtg5. Alizarin Red staining was carried out at 10 days (a) and 17 days (b) after infection, followed by dissolving the stains for quantitative absorbance measurement (c). Representative results are shown. “***” $P < 0.01$, compared with that of the Ad-BMP9 group.

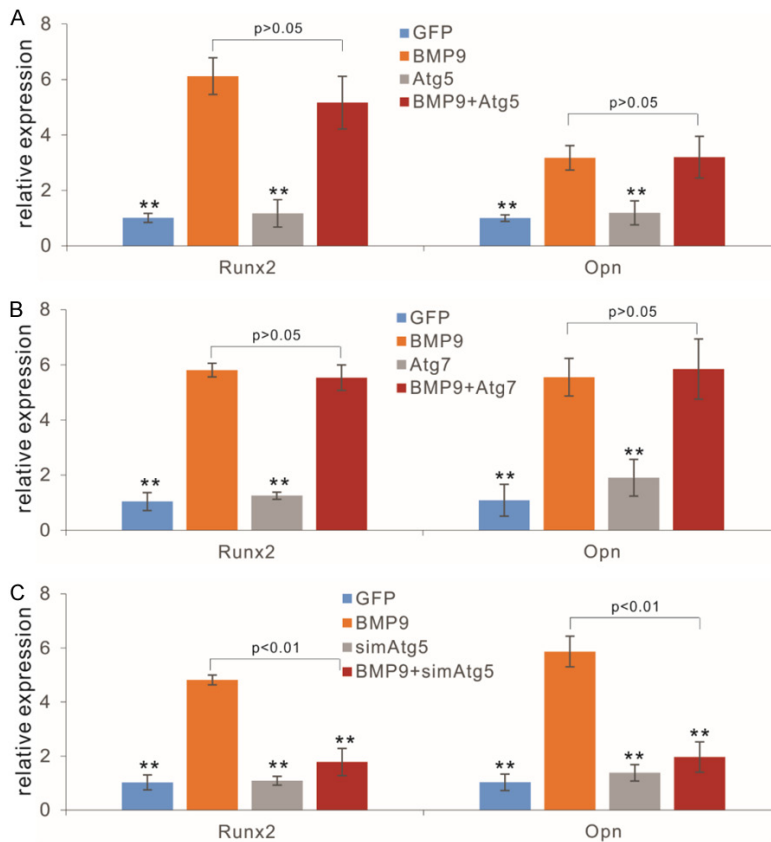


Figure 5. Silencing *Atg5* expression inhibits BMP9-induced expression of *Runx2* and osteopontin (*Opn*) in MSCs. Subconfluent MSCs were infected with Ad-GFP, Ad-BMP9, and/or Ad-ATG5 (A), Ad-ATG7 (B), or AdR-simAtg5 (C). Total RNA was isolated at 72 h after infection and subjected to RT-qPCR analysis of *Runx2* and *Opn* expression. “***” $P < 0.01$, compared with that of the Ad-BMP9 group.

BMP9+ATG5, BMP9+ATG7, BMP9 only, and BMP9+simAtg5 groups, where the average gross sizes (Figure 6Aa) and micro-CT 3D reconstructed images (Figure 6Ab) indicated that the bony masses retrieved from the BMP9+simAtg5 group were noticeably smaller than that from the BMP9 alone group, although masses from the ATG5 or ATG7 overexpression group had roughly similar sizes to that of the BMP9 alone group (Figure 6Aa, 6Ab). The micro-CT data were quantitatively analyzed and confirmed that silencing *Atg5* inhibited the average bone volume of the ectopic bone masses induced by BMP9 (Figure 6Ac).

Histologic analysis revealed that the masses retrieved from BMP9 alone, BMP9+ATG5,

BMP9+ATG7 groups exhibited similar bone histology with abundance of mature trabecular bone, whereas the BMP9+simAtg5 group lacked significant trabecular bone structure and only displayed immature osteoid matrix-like structure (Figure 6Ba). Trichrome staining also revealed that the masses retrieved from the BMP9 alone, BMP9+ATG5, BMP9+ATG7 groups contained abundant highly mineralized mature bone matrix, while the BMP9+simAtg5 group only exhibited immature osteoid matrix structure (Figure 6Bb). These findings further validate the *in vitro* results and strongly suggest that a functional autophagy pathway may play an essential role in mediating osteogenesis induced by BMP9 in MSCs.

Discussion

Through a systematic analysis of the osteogenic activities of 14 human BMPs, we identified BMP9 as one of

the most potent osteoinductive BMPs [19, 21, 25, 26, 28]. Furthermore, we demonstrated that BMP9 also induces adipogenic and chondrogenic differentiation in MSCs [19, 21, 28, 86]. Subsequently, we demonstrated that BMP9 binds to ALK1/2 type I receptors and regulates a panel of downstream target genes and noncoding RNAs, as well as cross-talking with several signaling pathways in MSCs [16, 18, 20, 31-37, 40, 41, 43-45, 104, 105]. Nonetheless, the exact mechanism underlying BMP9-regulated osteogenic differentiation of MSCs remains to be fully understood.

Emerging evidence indicates that autophagy may play critical roles in cell homeostasis and stress responses, including bone homeostasis

Autophagy participates in BMP9-induced osteogenesis

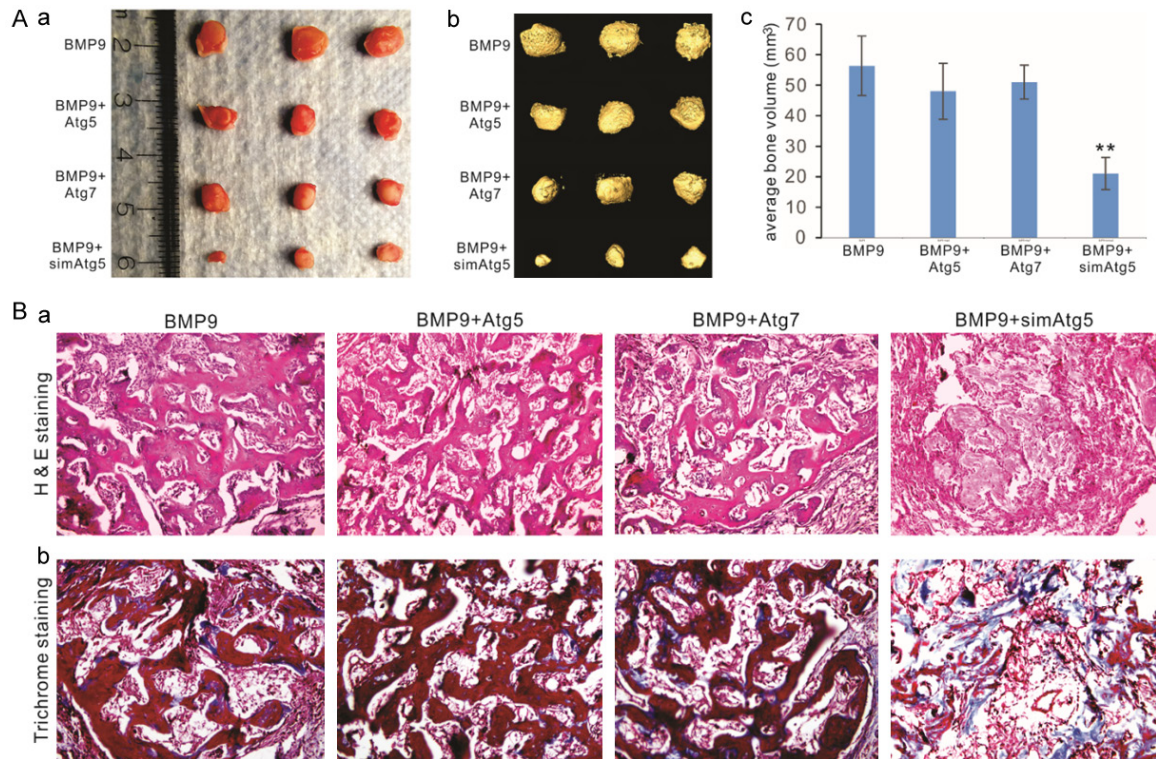


Figure 6. Silencing ATG5 inhibits BMP9-induced ectopic bone formation from MSCs. (A) Subconfluent MSCs were infected with Ad-GFP, Ad-BMP9, and/or Ad-ATG5, Ad-ATG7, or AdR-simAtg5 for 30 h, and collected for subcutaneous injection into the flanks of athymic nude mice. At 5 weeks, bony masses were harvested (Aa) and subjected to microCT imaging (Ab). No mass was recovered from the Ad-GFP control, Ad-ATG5 only, Ad-ATG7 only, and AdR-simAtg5 only groups. Representative images are shown. Micro-CT imaging data were used to calculate the average bone volume (Ac). “**” $P < 0.01$, compared with that of the Ad-BMP9 group. (B) The retrieved masses were decalcified, paraffin-embedded, and subjected to H, E staining (a) and trichrome staining (b). Representative images are shown.

[50-54]. In this study, we investigated whether or not autophagy plays any role in BMP9-induced osteogenic signaling. We found that autophagy blockade with chloroquine or silencing Atg5 effectively blocked BMP9-induced osteogenic differentiation of MSCs *in vitro* and *in vivo*, whereas overexpression of ATG5 or ATG7 did not enhance BMP9-induced osteogenic differentiation in MSCs. Our findings suggest that the basal autophagic activity may be sufficient for normal BMP9 osteogenic signaling, but a blockade of autophagic activity may effectively blunt BMP9 osteogenic signaling in MSCs. These findings should be consistent with the fact that paradoxical roles of autophagy in maintaining cell homeostasis and stress responses mandate a balanced autophagic activity in MSCs.

It was reported that autophagosomes were shown to accumulate in the stem state of MSCs and deliver them to lysosomes once differenti-

ation was initiated [106], and more differentiated osteocytes exhibited higher levels of autophagic flux [107]. Accordingly, osteocyte-specific suppression of autophagy was shown to mimic the skeletal aging phenotype [108]. Mice lacking Atg7 in osteoblasts had low bone mass and fractures, and were associated with reductions of both osteoclast and osteoblast numbers [109], further confirming that autophagy in osteoblasts may contribute to skeletal homeostasis. However, inhibition of autophagy in osteocytes did not reverse the glucocorticoids' adverse impact on cortical bone [110]. It was reported that Atg5 and Atg7 in mononuclear osteoclast progenitors were required for appropriate localization of lysosomes within the actin ring, as well as for the pit formation during bone resorption, although they were not required for osteoclastogenesis and osteoclast maturation [111]. Furthermore, cartilage-specific knockout of Atg7 in mice led to reduced chondrocyte proliferation and differentiation,

Autophagy participates in BMP9-induced osteogenesis

and increased chondrocyte apoptosis [112], consistent with the fact that autophagy is generally considered to be an important cell survival pathway.

In summary, we investigated if autophagy plays any role in BMP9-induced osteogenic signaling in MSCs. We found that autophagy blockade with chloroquine or silencing *Atg5* expression significantly diminished BMP9-induced osteogenic differentiation of MSCs both *in vitro* and *in vivo*, whereas overexpression of *ATG5* or *ATG7* did not enhance BMP9-induced osteogenic differentiation under the same conditions. Collectively, our findings strongly suggest that a functional autophagy pathway may play an essential role in mediating BMP9-induced osteogenesis of MSCs. Thus, it is conceivable that restoration of dysregulated autophagic activity in MSCs through a controlled delivery of BMP9 may be explored as a therapeutic strategy to treat bone fracture healing, bone defects, or osteoporosis.

Acknowledgements

The authors wish to thank Dr. Aaron Hsiu-Ming Tsai of the Integrated Small Animal Imaging Research Resource (iSAIRR) Faculty at The University of Chicago, for his valuable and resourceful support. The reported work was supported in part by research grants from the National Institutes of Health (CA226303 to TCH, DE030480 to RRR, and AR072731 to JY), the Chicago Biomedical Consortium with support from the Searle Funds at The Chicago Community Trust (RRR), and the Scoliosis Research Society (TCH and MJL). WW was supported by the Medical Scientist Training Program of the National Institutes of Health (T32 GM007281). This project was also supported in part by The University of Chicago Cancer Center Support Grant (P30CA014599) and the National Center for Advancing Translational Sciences (NCATS) of the National Institutes of Health (NIH) through Grant Number 5UL1TR002389-04 that funds the Institute for Translational Medicine (ITM). SHH and TCH were grateful for the support from the SHOCK Fund at The University of Chicago. TCH was supported by the Mabel Green Myers Research Endowment Fund and The University of Chicago Orthopaedics Alumni Fund. Funding sources were not involved in the study design; in the collection, analysis and/or interpretation of data;

in the writing of the report; or in the decision to submit the paper for publication.

Disclosure of conflict of interest

None.

Address correspondence to: Dr. Tong-Chuan He, Molecular Oncology Laboratory, Department of Orthopaedic Surgery and Rehabilitation Medicine, The University of Chicago Medical Center, 5841 South Maryland Avenue, MC3079, Chicago, IL 60637, USA. Tel: 773-702-7169; Fax: 773-834-4598; E-mail: tche@uchicago.edu; Dr. Yongtao Zhang, Department of Orthopaedic Surgery, The Affiliated Hospital of Qingdao University, Jiangsu Road #16, Shinan District, Qingdao 266061, China. Tel: +86-532-82913558; Fax: +86-532-82913558; E-mail: drzhang215@163.com

References

- [1] Pittenger MF, Discher DE, Peault BM, Phinney DG, Hare JM and Caplan AI. Mesenchymal stem cell perspective: cell biology to clinical progress. *NPJ Regen Med* 2019; 4: 22.
- [2] Caplan AI and Bruder SP. Mesenchymal stem cells: building blocks for molecular medicine in the 21st century. *Trends Mol Med* 2001; 7: 259-264.
- [3] Deng ZL, Sharff KA, Tang N, Song WX, Luo J, Luo X, Chen J, Bennett E, Reid R, Manning D, Xue A, Montag AG, Luu HH, Haydon RC and He TC. Regulation of osteogenic differentiation during skeletal development. *Front Biosci* 2008; 13: 2001-2021.
- [4] Rastegar F, Shenaq D, Huang J, Zhang W, Zhang BQ, He BC, Chen L, Zuo GW, Luo Q, Shi Q, Wagner ER, Huang E, Gao Y, Gao JL, Kim SH, Zhou JZ, Bi Y, Su Y, Zhu G, Luo J, Luo X, Qin J, Reid RR, Luu HH, Haydon RC, Deng ZL and He TC. Mesenchymal stem cells: molecular characteristics and clinical applications. *World J Stem Cells* 2010; 2: 67-80.
- [5] Shenaq DS, Rastegar F, Petkovic D, Zhang BQ, He BC, Chen L, Zuo GW, Luo Q, Shi Q, Wagner ER, Huang E, Gao Y, Gao JL, Kim SH, Yang K, Bi Y, Su Y, Zhu G, Luo J, Luo X, Qin J, Reid RR, Luu HH, Haydon RC and He TC. Mesenchymal progenitor cells and their orthopedic applications: forging a path towards clinical trials. *Stem Cells Int* 2010; 2010: 519028.
- [6] Teven CM, Liu X, Hu N, Tang N, Kim SH, Huang E, Yang K, Li M, Gao JL, Liu H, Natale RB, Luther G, Luo Q, Wang L, Rames R, Bi Y, Luo J, Luu HH, Haydon RC, Reid RR and He TC. Epigenetic regulation of mesenchymal stem cells: a focus on osteogenic and adipogenic differentiation. *Stem Cells Int* 2011; 2011: 201371.

Autophagy participates in BMP9-induced osteogenesis

- [7] Raucci A, Bellosta P, Grassi R, Basilico C and Mansukhani A. Osteoblast proliferation or differentiation is regulated by relative strengths of opposing signaling pathways. *J Cell Physiol* 2008; 215: 442-451.
- [8] Kim JH, Liu X, Wang J, Chen X, Zhang H, Kim SH, Cui J, Li R, Zhang W, Kong Y, Zhang J, Shui W, Lamplot J, Rogers MR, Zhao C, Wang N, Rajan P, Tomal J, Statz J, Wu N, Luu HH, Haydon RC and He TC. Wnt signaling in bone formation and its therapeutic potential for bone diseases. *Ther Adv Musculoskelet Dis* 2013; 5: 13-31.
- [9] Yang K, Wang X, Zhang H, Wang Z, Nan G, Li Y, Zhang F, Mohammed MK, Haydon RC, Luu HH, Bi Y and He TC. The evolving roles of canonical WNT signaling in stem cells and tumorigenesis: implications in targeted cancer therapies. *Lab Invest* 2016; 96: 116-136.
- [10] Denduluri SK, Idowu O, Wang Z, Liao Z, Yan Z, Mohammed MK, Ye J, Wei Q, Wang J, Zhao L and Luu HH. Insulin-like growth factor (IGF) signaling in tumorigenesis and the development of cancer drug resistance. *Genes Dis* 2015; 2: 13-25.
- [11] Teven CM, Farina EM, Rivas J and Reid RR. Fibroblast growth factor (FGF) signaling in development and skeletal diseases. *Genes Dis* 2014; 1: 199-213.
- [12] Jo A, Denduluri S, Zhang B, Wang Z, Yin L, Yan Z, Kang R, Shi LL, Mok J, Lee MJ and Haydon RC. The versatile functions of Sox9 in development, stem cells, and human diseases. *Genes Dis* 2014; 1: 149-161.
- [13] Louvi A and Artavanis-Tsakonas S. Notch and disease: a growing field. *Semin Cell Dev Biol* 2012; 23: 473-480.
- [14] Zanotti S and Canalis E. Notch and the skeleton. *Mol Cell Biol* 2010; 30: 886-896.
- [15] Guruharsha KG, Kankel MW and Artavanis-Tsakonas S. The Notch signalling system: recent insights into the complexity of a conserved pathway. *Nat Rev Genet* 2012; 13: 654-666.
- [16] Zhang F, Song J, Zhang H, Huang E, Song D, Tollemar V, Wang J, Wang J, Mohammed M, Wei Q, Fan J, Liao J, Zou Y, Liu F, Hu X, Qu X, Chen L, Yu X, Luu HH, Lee MJ, He TC and Ji P. Wnt and BMP signaling crosstalk in regulating dental stem cells: implications in dental tissue engineering. *Genes Dis* 2016; 3: 263-276.
- [17] Zhang L, Luo Q, Shu Y, Zeng Z, Huang B, Feng Y, Zhang B, Wang X, Lei Y, Ye Z, Zhao L, Cao D, Yang L, Chen X, Liu B, Wagstaff W, Reid RR, Luu HH, Haydon RC, Lee MJ, Wolf JM, Fu Z, He TC and Kang Q. Transcriptomic landscape regulated by the 14 types of bone morphogenetic proteins (BMPs) in lineage commitment and differentiation of mesenchymal stem cells (MSCs). *Genes Dis* 2019; 6: 258-275.
- [18] Pakvasa M, Haravu P, Boachie-Mensah M, Jones A, Coalson E, Liao J, Zeng Z, Wu D, Qin K, Wu X, Luo H, Zhang J, Zhang M, He F, Mao Y, Zhang Y, Niu C, Wu M, Zhao X, Wang H, Huang L, Shi D, Liu Q, Ni N, Fu K, Lee MJ, Wolf JM, Athiviraham A, Ho SS, He TC, Hynes K, Strelzow J, El Dafrawy M and Reid RR. Notch signaling: its essential roles in bone and craniofacial development. *Genes Dis* 2021; 8: 8-24.
- [19] Luu HH, Song WX, Luo X, Manning D, Luo J, Deng ZL, Sharff KA, Montag AG, Haydon RC and He TC. Distinct roles of bone morphogenetic proteins in osteogenic differentiation of mesenchymal stem cells. *J Orthop Res* 2007; 25: 665-677.
- [20] Wang RN, Green J, Wang Z, Deng Y, Qiao M, Peabody M, Zhang Q, Ye J, Yan Z, Denduluri S, Idowu O, Li M, Shen C, Hu A, Haydon RC, Kang R, Mok J, Lee MJ, Luu HH and Shi LL. Bone Morphogenetic Protein (BMP) signaling in development and human diseases. *Genes Dis* 2014; 1: 87-105.
- [21] Mostafa S, Pakvasa M, Coalson E, Zhu A, Alverdy A, Castillo H, Fan J, Li A, Feng Y, Wu D, Bishop E, Du S, Spezia M, Li A, Hagag O, Deng A, Liu W, Li M, Ho SS, Athiviraham A, Lee MJ, Wolf JM, Ameer GA, Luu HH, Haydon RC, Strelzow J, Hynes K, He TC and Reid RR. The wonders of BMP9: from mesenchymal stem cell differentiation, angiogenesis, neurogenesis, tumorigenesis, and metabolism to regenerative medicine. *Genes Dis* 2019; 6: 201-223.
- [22] Reddi AH. Role of morphogenetic proteins in skeletal tissue engineering and regeneration. *Nat Biotechnol* 1998; 16: 247-252.
- [23] Zou H, Choe KM, Lu Y, Massague J and Niswander L. BMP signaling and vertebrate limb development. *Cold Spring Harb Symp Quant Biol* 1997; 62: 269-272.
- [24] Liu W, Deng Z, Zeng Z, Fan J, Feng Y, Wang X, Cao D, Zhang B, Yang L, Liu B, Pakvasa M, Wagstaff W, Wu X, Luo H, Zhang J, Zhang M, He F, Mao Y, Ding H, Zhang Y, Niu C, Haydon RC, Luu HH, Wolf JM, Lee MJ, Huang W, He TC and Zou Y. Highly expressed BMP9/GDF2 in postnatal mouse liver and lungs may account for its pleiotropic effects on stem cell differentiation, angiogenesis, tumor growth and metabolism. *Genes Dis* 2020; 7: 235-244.
- [25] Cheng H, Jiang W, Phillips FM, Haydon RC, Peng Y, Zhou L, Luu HH, An N, Breyer B, Vanichakarn P, Szatkowski JP, Park JY and He TC. Osteogenic activity of the fourteen types of human bone morphogenetic proteins (BMPs). *J Bone Joint Surg Am* 2003; 85: 1544-1552.
- [26] Kang Q, Sun MH, Cheng H, Peng Y, Montag AG, Deyrup AT, Jiang W, Luu HH, Luo J, Szatkowski JP, Vanichakarn P, Park JY, Li Y, Haydon RC and He TC. Characterization of the distinct orthotopic bone-forming activity of 14 BMPs using

Autophagy participates in BMP9-induced osteogenesis

- recombinant adenovirus-mediated gene delivery. *Gene Ther* 2004; 11: 1312-1320.
- [27] Luther G, Wagner ER, Zhu G, Kang Q, Luo Q, Lamplot J, Bi Y, Luo X, Luo J, Teven C, Shi Q, Kim SH, Gao JL, Huang E, Yang K, Rames R, Liu X, Li M, Hu N, Liu H, Su Y, Chen L, He BC, Zuo GW, Deng ZL, Reid RR, Luu HH, Haydon RC and He TC. BMP-9 induced osteogenic differentiation of mesenchymal stem cells: molecular mechanism and therapeutic potential. *Curr Gene Ther* 2011; 11: 229-240.
- [28] Lamplot JD, Qin J, Nan G, Wang J, Liu X, Yin L, Tomal J, Li R, Shui W, Zhang H, Kim SH, Zhang W, Zhang J, Kong Y, Denduluri S, Rogers MR, Pratt A, Haydon RC, Luu HH, Angeles J, Shi LL and He TC. BMP9 signaling in stem cell differentiation and osteogenesis. *Am J Stem Cells* 2013; 2: 1-21.
- [29] Wang Y, Hong S, Li M, Zhang J, Bi Y, He Y, Liu X, Nan G, Su Y, Zhu G, Li R, Zhang W, Wang J, Zhang H, Kong Y, Shui W, Wu N, He Y, Chen X, Luu HH, Haydon RC, Shi LL, He TC and Qin J. Noggin resistance contributes to the potent osteogenic capability of BMP9 in mesenchymal stem cells. *J Orthop Res* 2013; 31: 1796-1803.
- [30] Luo J, Tang M, Huang J, He BC, Gao JL, Chen L, Zuo GW, Zhang W, Luo Q, Shi Q, Zhang BQ, Bi Y, Luo X, Jiang W, Su Y, Shen J, Kim SH, Huang E, Gao Y, Zhou JZ, Yang K, Luu HH, Pan X, Haydon RC, Deng ZL and He TC. TGFbeta/BMP type I receptors ALK1 and ALK2 are essential for BMP9-induced osteogenic signaling in mesenchymal stem cells. *J Biol Chem* 2010; 285: 29588-29598.
- [31] Peng Y, Kang Q, Cheng H, Li X, Sun MH, Jiang W, Luu HH, Park JY, Haydon RC and He TC. Transcriptional characterization of bone morphogenetic proteins (BMPs)-mediated osteogenic signaling. *J Cell Biochem* 2003; 90: 1149-1165.
- [32] Peng Y, Kang Q, Luo Q, Jiang W, Si W, Liu BA, Luu HH, Park JK, Li X, Luo J, Montag AG, Haydon RC and He TC. Inhibitor of DNA binding/differentiation helix-loop-helix proteins mediate bone morphogenetic protein-induced osteoblast differentiation of mesenchymal stem cells. *J Biol Chem* 2004; 279: 32941-32949.
- [33] Luo Q, Kang Q, Si W, Jiang W, Park JK, Peng Y, Li X, Luu HH, Luo J, Montag AG, Haydon RC and He TC. Connective tissue growth factor (CTGF) is regulated by Wnt and bone morphogenetic proteins signaling in osteoblast differentiation of mesenchymal stem cells. *J Biol Chem* 2004; 279: 55958-55968.
- [34] Sharff KA, Song WX, Luo X, Tang N, Luo J, Chen J, Bi Y, He BC, Huang J, Li X, Jiang W, Zhu GH, Su Y, He Y, Shen J, Wang Y, Chen L, Zuo GW, Liu B, Pan X, Reid RR, Luu HH, Haydon RC and He TC. Hey1 basic helix-loop-helix protein plays an important role in mediating BMP9-induced osteogenic differentiation of mesenchymal progenitor cells. *J Biol Chem* 2009; 284: 649-659.
- [35] Huang E, Zhu G, Jiang W, Yang K, Gao Y, Luo Q, Gao JL, Kim SH, Liu X, Li M, Shi Q, Hu N, Wang L, Liu H, Cui J, Zhang W, Li R, Chen X, Kong YH, Zhang J, Wang J, Shen J, Bi Y, Statz J, He BC, Luo J, Wang H, Xiong F, Luu HH, Haydon RC, Yang L and He TC. Growth hormone synergizes with BMP9 in osteogenic differentiation by activating the JAK/STAT/IGF1 pathway in murine multilineage cells. *J Bone Miner Res* 2012; 27: 1566-1575.
- [36] Wang J, Liao J, Zhang F, Song D, Lu M, Liu J, Wei Q, Tang S, Liu H, Fan J, Zou Y, Guo D, Huang J, Liu F, Ma C, Hu X, Li L, Qu X, Chen L, Weng Y, Lee MJ, He TC, Reid RR and Zhang J. NEL-like molecule-1 (Nell1) is regulated by bone morphogenetic protein 9 (BMP9) and potentiates BMP9-induced osteogenic differentiation at the expense of adipogenesis in mesenchymal stem cells. *Cell Physiol Biochem* 2017; 41: 484-500.
- [37] Wang J, Zhang H, Zhang W, Huang E, Wang N, Wu N, Wen S, Chen X, Liao Z, Deng F, Yin L, Zhang J, Zhang Q, Yan Z, Liu W, Zhang Z, Ye J, Deng Y, Luu HH, Haydon RC, He TC and Deng F. Bone morphogenetic protein-9 effectively induces osteo/odontoblastic differentiation of the reversibly immortalized stem cells of dental apical papilla. *Stem Cells Dev* 2014; 23: 1405-1416.
- [38] Si W, Kang Q, Luu HH, Park JK, Luo Q, Song WX, Jiang W, Luo X, Li X, Yin H, Montag AG, Haydon RC and He TC. CCN1/Cyr61 is regulated by the canonical Wnt signal and plays an important role in Wnt3A-induced osteoblast differentiation of mesenchymal stem cells. *Mol Cell Biol* 2006; 26: 2955-2964.
- [39] Liao J, Yu X, Hu X, Fan J, Wang J, Zhang Z, Zhao C, Zeng Z, Shu Y, Zhang R, Yan S, Li Y, Zhang W, Cui J, Ma C, Li L, Yu Y, Wu T, Wu X, Lei J, Wang J, Yang C, Wu K, Wu Y, Tang J, He BC, Deng ZL, Luu HH, Haydon RC, Reid RR, Lee MJ, Wolf JM, Huang W and He TC. lncRNA H19 mediates BMP9-induced osteogenic differentiation of mesenchymal stem cells (MSCs) through Notch signaling. *Oncotarget* 2017; 8: 53581-53601.
- [40] Zhang Z, Liu J, Zeng Z, Fan J, Huang S, Zhang L, Zhang B, Wang X, Feng Y, Ye Z, Zhao L, Cao D, Yang L, Pakvasa M, Liu B, Wagstaff W, Wu X, Luo H, Zhang J, Zhang M, He F, Mao Y, Ding H, Zhang Y, Niu C, Haydon RC, Luu HH, Lee MJ, Wolf JM, Shao Z and He TC. lncRNA Rmst acts as an important mediator of BMP9-induced osteogenic differentiation of mesenchymal stem

Autophagy participates in BMP9-induced osteogenesis

- cells (MSCs) by antagonizing Notch-targeting microRNAs. *Aging* (Albany NY) 2019; 11: 12476-12496.
- [41] Li R, Zhang W, Yan Z, Liu W, Fan J, Feng Y, Zeng Z, Cao D, Haydon RC, Luu HH, Deng ZL, He TC and Zou Y. Long non-coding RNA (LncRNA) HO-TAIR regulates BMP9-induced osteogenic differentiation by targeting the proliferation of mesenchymal stem cells (MSCs). *Aging* (Albany NY) 2021; 13: 4199-4214
- [42] Tang N, Song WX, Luo J, Luo X, Chen J, Sharff KA, Bi Y, He BC, Huang JY, Zhu GH, Su YX, Jiang W, Tang M, He Y, Wang Y, Chen L, Zuo GW, Shen J, Pan X, Reid RR, Luu HH, Haydon RC and He TC. BMP-9-induced osteogenic differentiation of mesenchymal progenitors requires functional canonical Wnt/beta-catenin signaling. *J Cell Mol Med* 2009; 13: 2448-2464.
- [43] Zhang W, Deng ZL, Chen L, Zuo GW, Luo Q, Shi Q, Zhang BQ, Wagner ER, Rastegar F, Kim SH, Jiang W, Shen J, Huang E, Gao Y, Gao JL, Zhou JZ, Luo J, Huang J, Luo X, Bi Y, Su Y, Yang K, Liu H, Luu HH, Haydon RC, He TC and He BC. Retinoic acids potentiate BMP9-induced osteogenic differentiation of mesenchymal progenitor cells. *PLoS One* 2010; 5: e11917.
- [44] Zhang H, Wang J, Deng F, Huang E, Yan Z, Wang Z, Deng Y, Zhang Q, Zhang Z, Ye J, Qiao M, Li R, Wang J, Wei Q, Zhou G, Luu HH, Haydon RC, He TC and Deng F. Canonical Wnt signaling acts synergistically on BMP9-induced osteo/odontoblastic differentiation of stem cells of dental apical papilla (SCAPs). *Biomaterials* 2015; 39: 145-154.
- [45] Liao J, Wei Q, Zou Y, Fan J, Song D, Cui J, Zhang W, Zhu Y, Ma C, Hu X, Qu X, Chen L, Yu X, Zhang Z, Wang C, Zhao C, Zeng Z, Zhang R, Yan S, Wu T, Wu X, Shu Y, Lei J, Li Y, Luu HH, Lee MJ, Reid RR, Ameer GA, Wolf JM, He TC and Huang W. Notch signaling augments BMP9-induced bone formation by promoting the osteogenesis-angiogenesis coupling process in mesenchymal stem cells (MSCs). *Cell Physiol Biochem* 2017; 41: 1905-1923.
- [46] Cui J, Zhang W, Huang E, Wang J, Liao J, Li R, Yu X, Zhao C, Zeng Z, Shu Y, Zhang R, Yan S, Lei J, Yang C, Wu K, Wu Y, Huang S, Ji X, Li A, Gong C, Yuan C, Zhang L, Liu W, Huang B, Feng Y, An L, Zhang B, Dai Z, Shen Y, Luo W, Wang X, Huang A, Luu HH, Reid RR, Wolf JM, Thinakaran G, Lee MJ and He TC. BMP9-induced osteoblastic differentiation requires functional Notch signaling in mesenchymal stem cells. *Lab Invest* 2019; 99: 58-71.
- [47] Zhang B, Yang L, Zeng Z, Feng Y, Wang X, Wu X, Luo H, Zhang J, Zhang M, Pakvasa M, Wagstaff W, He F, Mao Y, Qin D, Ding H, Zhang Y, Niu C, Wu M, Zhao X, Wang H, Huang L, Shi D, Liu Q, Ni N, Fu K, Athiviraham A, Moriatis Wolf J, Lee MJ, Hynes K, Strelzow J, El Dafrawy M, Xia Y and He TC. Leptin potentiates BMP9-induced osteogenic differentiation of mesenchymal stem cells through the activation of JAK/STAT signaling. *Stem Cells Dev* 2020; 29: 498-510.
- [48] Huang X, Chen Q, Luo W, Pakvasa M, Zhang Y, Zheng L, Li S, Yang Z, Zeng H, Liang F, Zhang F, Hu DA, Qin KH, Wang EJ, Qin DS, Reid RR, He TC, Athiviraham A, El Dafrawy M and Zhang H. SATB2: a versatile transcriptional regulator of craniofacial and skeleton development, neurogenesis and tumorigenesis, and its applications in regenerative medicine. *Genes Dis* 2020.
- [49] Luo W, Zhang L, Huang B, Zhang H, Zhang Y, Zhang F, Liang P, Chen Q, Cheng Q, Tan D, Tan Y, Song J, Zhao T, Haydon RC, Reid RR, Luu HH, Lee MJ, El Dafrawy M, Ji P, He TC and Gou L. BMP9-initiated osteogenic/odontogenic differentiation of mouse tooth germ mesenchymal cells (TGMCS) requires Wnt/beta-catenin signalling activity. *J Cell Mol Med* 2021; 25: 2666-2678.
- [50] Guo YF, Su T, Yang M, Li CJ, Guo Q, Xiao Y, Huang Y, Liu Y and Luo XH. The role of autophagy in bone homeostasis. *J Cell Physiol* 2021; 236: 4152-4173.
- [51] Jaber FA, Khan NM, Ansari MY, Al-Adlaan AA, Hussein NJ and Safadi FF. Autophagy plays an essential role in bone homeostasis. *J Cell Physiol* 2019; 234: 12105-12115.
- [52] Yin X, Zhou C, Li J, Liu R, Shi B, Yuan Q and Zou S. Autophagy in bone homeostasis and the onset of osteoporosis. *Bone Res* 2019; 7: 28.
- [53] Bento CF, Renna M, Ghislat G, Puri C, Ashkenazi A, Vicinanza M, Menzies FM and Rubinsztein DC. Mammalian autophagy: how does it work? *Annu Rev Biochem* 2016; 85: 685-713.
- [54] Dikic I and Elazar Z. Mechanism and medical implications of mammalian autophagy. *Nat Rev Mol Cell Biol* 2018; 19: 349-364.
- [55] Gelman A and Elazar Z. Autophagic factors cut to the bone. *Dev Cell* 2011; 21: 808-810.
- [56] Hu X, Li L, Yu X, Zhang R, Yan S, Zeng Z, Shu Y, Zhao C, Wu X, Lei J, Li Y, Zhang W, Yang C, Wu K, Wu Y, An L, Huang S, Ji X, Gong C, Yuan C, Zhang L, Liu W, Huang B, Feng Y, Zhang B, Haydon RC, Luu HH, Reid RR, Lee MJ, Wolf JM, Yu Z and He TC. CRISPR/Cas9-mediated reversibly immortalized mouse bone marrow stromal stem cells (BMSCs) retain multipotent features of mesenchymal stem cells (MSCs). *Oncotarget* 2017; 8: 111847-111865.
- [57] Wu N, Zhang H, Deng F, Li R, Zhang W, Chen X, Wen S, Wang N, Zhang J, Yin L, Liao Z, Zhang Z, Zhang Q, Yan Z, Liu W, Wu D, Ye J, Deng Y, Yang K, Luu HH, Haydon RC and He TC. Overexpression of Ad5 precursor terminal protein accelerates recombinant adenovirus packaging and amplification in HEK-293 packaging cells. *Gene Ther* 2014; 21: 629-637.

Autophagy participates in BMP9-induced osteogenesis

- [58] Wei Q, Fan J, Liao J, Zou Y, Song D, Liu J, Cui J, Liu F, Ma C, Hu X, Li L, Yu Y, Qu X, Chen L, Yu X, Zhang Z, Zhao C, Zeng Z, Zhang R, Yan S, Wu X, Shu Y, Reid RR, Lee MJ, Wolf JM and He TC. Engineering the rapid adenovirus production and amplification (RAPA) cell line to expedite the generation of recombinant adenoviruses. *Cell Physiol Biochem* 2017; 41: 2383-2398.
- [59] Zeng Z, Huang B, Huang S, Zhang R, Yan S, Yu X, Shu Y, Zhao C, Lei J, Zhang W, Yang C, Wu K, Wu Y, An L, Ji X, Gong C, Yuan C, Zhang L, Liu W, Feng Y, Zhang B, Dai Z, Shen Y, Wang X, Luo W, Haydon RC, Luu HH, Zhou L, Reid RR, He TC and Wu X. The development of a sensitive fluorescent protein-based transcript reporter for high throughput screening of negative modulators of lncRNAs. *Genes Dis* 2018; 5: 62-74.
- [60] Cao D, Lei Y, Ye Z, Zhao L, Wang H, Zhang J, He F, Huang L, Shi D, Liu Q, Ni N, Pakvasa M, Wagstaff W, Zhao X, Fu K, Tucker AB, Chen C, Reid RR, Haydon RC, Luu HH, He TC and Liao Z. Blockade of IGF/IGF-1R signaling axis with soluble IGF-1R mutants suppresses the cell proliferation and tumor growth of human osteosarcoma. *Am J Cancer Res* 2020; 10: 3248-3266.
- [61] Huang B, Huang LF, Zhao L, Zeng Z, Wang X, Cao D, Yang L, Ye Z, Chen X, Liu B, He TC and Wang X. Microvesicles (MVs) secreted from adipose-derived stem cells (ADSCs) contain multiple microRNAs and promote the migration and invasion of endothelial cells. *Genes Dis* 2020; 7: 225-234.
- [62] Zhao L, Huang L, Zhang J, Fan J, He F, Zhao X, Wang H, Liu Q, Shi D, Ni N, Wagstaff W, Pakvasa M, Fu K, Tucker AB, Chen C, Reid RR, Haydon RC, Luu HH, Shen L, Qi H and He TC. The inhibition of BRAF activity sensitizes chemoresistant human ovarian cancer cells to paclitaxel-induced cytotoxicity and tumor growth inhibition. *Am J Transl Res* 2020; 12: 8084-8098.
- [63] Fan J, Feng Y, Zhang R, Zhang W, Shu Y, Zeng Z, Huang S, Zhang L, Huang B, Wu D, Zhang B, Wang X, Lei Y, Ye Z, Zhao L, Cao D, Yang L, Chen X, Liu B, Wagstaff W, He F, Wu X, Zhang J, Moriatis Wolf J, Lee MJ, Haydon RC, Luu HH, Huang A, He TC and Yan S. A simplified system for the effective expression and delivery of functional mature microRNAs in mammalian cells. *Cancer Gene Ther* 2020; 27: 424-437.
- [64] He TC. Adenoviral vectors. Adenoviral vectors in current protocols in human genetics. New York: John Wiley & Sons, Inc.; 2004. pp. 12.14.11-12.14.25.
- [65] Luo J, Deng ZL, Luo X, Tang N, Song WX, Chen J, Sharff KA, Luu HH, Haydon RC, Kinzler KW, Vogelstein B and He TC. A protocol for rapid generation of recombinant adenoviruses using the AdEasy system. *Nat Protoc* 2007; 2: 1236-1247.
- [66] Lee CS, Bishop ES, Zhang R, Yu X, Farina EM, Yan S, Zhao C, Zheng Z, Shu Y, Wu X, Lei J, Li Y, Zhang W, Yang C, Wu K, Wu Y, Ho S, Athiviraham A, Lee MJ, Wolf JM, Reid RR and He TC. Adenovirus-mediated gene delivery: potential applications for gene and cell-based therapies in the new era of personalized medicine. *Genes Dis* 2017; 4: 43-63.
- [67] He F, Ni N, Zeng Z, Wu D, Feng Y, Li AJ, Luu B, Li AF, Qin K, Wang E, Wang X, Wu X, Luo H, Zhang J, Zhang M, Mao Y, Pakvasa M, Wagstaff W, Zhang Y, Niu C, Wang H, Huang L, Shi D, Liu Q, Zhao X, Fu K, Reid RR, Wolf JM, Lee MJ, Hynes K, Strelzow J, El Dafrawy M, Gan H, He TC and Fan J. FAMS: a synthetic biology approach to the fast assembly of multiplex siRNAs for silencing gene expression in mammalian cells. *Mol Ther Nucleic Acids* 2020; 22: 885-899.
- [68] Luo Q, Kang Q, Song WX, Luu HH, Luo X, An N, Luo J, Deng ZL, Jiang W, Yin H, Chen J, Sharff KA, Tang N, Bennett E, Haydon RC and He TC. Selection and validation of optimal siRNA target sites for RNAi-mediated gene silencing. *Gene* 2007; 395: 160-169.
- [69] Deng F, Chen X, Liao Z, Yan Z, Wang Z, Deng Y, Zhang Q, Zhang Z, Ye J, Qiao M, Li R, Denduluri S, Wang J, Wei Q, Li M, Geng N, Zhao L, Zhou G, Zhang P, Luu HH, Haydon RC, Reid RR, Yang T and He TC. A simplified and versatile system for the simultaneous expression of multiple siRNAs in mammalian cells using Gibson DNA assembly. *PLoS One* 2014; 9: e113064.
- [70] Wang X, Yuan C, Huang B, Fan J, Feng Y, Li AJ, Zhang B, Lei Y, Ye Z, Zhao L, Cao D, Yang L, Wu D, Chen X, Liu B, Wagstaff W, He F, Wu X, Luo H, Zhang J, Zhang M, Haydon RC, Luu HH, Lee MJ, Moriatis Wolf J, Huang A, He TC and Zeng Z. Developing a versatile shotgun cloning strategy for single-vector-based multiplex expression of short interfering RNAs (siRNAs) in mammalian cells. *ACS Synth Biol* 2019; 8: 2092-2105.
- [71] Wang X, Zhao L, Wu X, Luo H, Wu D, Zhang M, Zhang J, Pakvasa M, Wagstaff W, He F, Mao Y, Zhang Y, Niu C, Wu M, Zhao X, Wang H, Huang L, Shi D, Liu Q, Ni N, Fu K, Hynes K, Strelzow J, El Dafrawy M, He TC, Qi H and Zeng Z. Development of a simplified and inexpensive RNA depletion method for plasmid DNA purification using size selection magnetic beads (SSMBs). *Genes Dis* 2020.
- [72] Wang N, Zhang H, Zhang BQ, Liu W, Zhang Z, Qiao M, Zhang H, Deng F, Wu N, Chen X, Wen S, Zhang J, Liao Z, Zhang Q, Yan Z, Yin L, Ye J, Deng Y, Luu HH, Haydon RC, Liang H and He TC. Adenovirus-mediated efficient gene transfer into cultured three-dimensional organoids. *PLoS One* 2014; 9: e93608.
- [73] Yan S, Zhang R, Wu K, Cui J, Huang S, Ji X, An L, Yuan C, Gong C, Zhang L, Liu W, Feng Y, Zhang B, Dai Z, Shen Y, Wang X, Luo W, Liu B, Haydon RC, Lee MJ, Reid RR, Wolf JM, Shi Q, Luu HH, He TC and Weng Y. Characterization of

Autophagy participates in BMP9-induced osteogenesis

- the essential role of bone morphogenetic protein 9 (BMP9) in osteogenic differentiation of mesenchymal stem cells (MSCs) through RNA interference. *Genes Dis* 2018; 5: 172-184.
- [74] Song D, Huang S, Zhang L, Liu W, Huang B, Feng Y, Liu B, He TC, Huang D and Reid RR. Differential responsiveness to BMP9 between patent and fused suture progenitor cells from craniosynostosis patients. *Plast Reconstr Surg* 2020; 145: 552e-562e.
- [75] Song D, Zhang F, Reid RR, Ye J, Wei Q, Liao J, Zou Y, Fan J, Ma C, Hu X, Qu X, Chen L, Li L, Yu Y, Yu X, Zhang Z, Zhao C, Zeng Z, Zhang R, Yan S, Wu T, Wu X, Shu Y, Lei J, Li Y, Zhang W, Wang J, Lee MJ, Wolf JM, Huang D and He TC. BMP9 induces osteogenesis and adipogenesis in the immortalized human cranial suture progenitors from the patent sutures of craniosynostosis patients. *J Cell Mol Med* 2017; 21: 2782-2795.
- [76] Shu Y, Wu K, Zeng Z, Huang S, Ji X, Yuan C, Zhang L, Liu W, Huang B, Feng Y, Zhang B, Dai Z, Shen Y, Luo W, Wang X, Liu B, Lei Y, Ye Z, Zhao L, Cao D, Yang L, Chen X, Luu HH, Reid RR, Wolf JM, Lee MJ and He TC. A simplified system to express circularized inhibitors of miRNA for stable and potent suppression of miRNA functions. *Mol Ther Nucleic Acids* 2018; 13: 556-567.
- [77] Denduluri SK, Scott B, Lamplot JD, Yin L, Yan Z, Wang Z, Ye J, Wang J, Wei Q, Mohammed MK, Haydon RC, Kang RW, He TC, Athiviraham A, Ho SH and Shi LL. Immortalized mouse achilles tenocytes demonstrate long-term proliferative capacity while retaining tenogenic properties. *Tissue Eng Part C Methods* 2016; 22: 280-289.
- [78] Zhao C, Wu N, Deng F, Zhang H, Wang N, Zhang W, Chen X, Wen S, Zhang J, Yin L, Liao Z, Zhang Z, Zhang Q, Yan Z, Liu W, Wu D, Ye J, Deng Y, Zhou G, Luu HH, Haydon RC, Si W and He TC. Adenovirus-mediated gene transfer in mesenchymal stem cells can be significantly enhanced by the cationic polymer polybrene. *PLoS One* 2014; 9: e92908.
- [79] Zhang Q, Wang J, Deng F, Yan Z, Xia Y, Wang Z, Ye J, Deng Y, Zhang Z, Qiao M, Li R, Denduluri SK, Wei Q, Zhao L, Lu S, Wang X, Tang S, Liu H, Luu HH, Haydon RC, He TC and Jiang L. TqPCR: a touchdown qPCR assay with significantly improved detection sensitivity and amplification efficiency of SYBR green qPCR. *PLoS One* 2015; 10: e0132666.
- [80] Liao J, Wei Q, Fan J, Zou Y, Song D, Liu J, Liu F, Ma C, Hu X, Li L, Yu Y, Qu X, Chen L, Yu X, Zhang Z, Zhao C, Zeng Z, Zhang R, Yan S, Wu T, Wu X, Shu Y, Lei J, Li Y, Zhang W, Wang J, Reid RR, Lee MJ, Huang W, Wolf JM, He TC and Wang J. Characterization of retroviral infectivity and superinfection resistance during retrovirus-mediated transduction of mammalian cells. *Gene Ther* 2017; 24: 333-341.
- [81] Fan J, Wei Q, Liao J, Zou Y, Song D, Xiong D, Ma C, Hu X, Qu X, Chen L, Li L, Yu Y, Yu X, Zhang Z, Zhao C, Zeng Z, Zhang R, Yan S, Wu T, Wu X, Shu Y, Lei J, Li Y, Zhang W, Haydon RC, Luu HH, Huang A, He TC and Tang H. Noncanonical Wnt signaling plays an important role in modulating canonical Wnt-regulated stemness, proliferation and terminal differentiation of hepatic progenitors. *Oncotarget* 2017; 8: 27105-27119.
- [82] Zeng Z, Huang B, Wang X, Fan J, Zhang B, Yang L, Feng Y, Wu X, Luo H, Zhang J, Zhang M, He F, Mao Y, Pakvasa M, Wagstaff W, Li AJ, Liu B, Ding H, Zhang Y, Niu C, Wu M, Zhao X, Wolf JM, Lee MJ, Huang A, Luu HH, Haydon RC and He TC. A reverse transcriptase-mediated ribosomal RNA depletion (RTR2D) strategy for the cost-effective construction of RNA sequencing libraries. *J Adv Res* 2020; 24: 239-250.
- [83] Huang E, Bi Y, Jiang W, Luo X, Yang K, Gao JL, Gao Y, Luo Q, Shi Q, Kim SH, Liu X, Li M, Hu N, Liu H, Cui J, Zhang W, Li R, Chen X, Shen J, Kong Y, Zhang J, Wang J, Luo J, He BC, Wang H, Reid RR, Luu HH, Haydon RC, Yang L and He TC. Conditionally immortalized mouse embryonic fibroblasts retain proliferative activity without compromising multipotent differentiation potential. *PLoS One* 2012; 7: e32428.
- [84] Li Y, Wagner ER, Yan Z, Wang Z, Luther G, Jiang W, Ye J, Wei Q, Wang J, Zhao L, Lu S, Wang X, Mohammed MK, Tang S, Liu H, Fan J, Zhang F, Zou Y, Song D, Liao J, Haydon RC, Luu HH and He TC. The calcium-binding protein S100A6 accelerates human osteosarcoma growth by promoting cell proliferation and inhibiting osteogenic differentiation. *Cell Physiol Biochem* 2015; 37: 2375-2392.
- [85] Li R, Zhang W, Cui J, Shui W, Yin L, Wang Y, Zhang H, Wang N, Wu N, Nan G, Chen X, Wen S, Deng F, Zhang H, Zhou G, Liao Z, Zhang J, Zhang Q, Yan Z, Liu W, Zhang Z, Ye J, Deng Y, Luu HH, Haydon RC, He TC and Deng ZL. Targeting BMP9-promoted human osteosarcoma growth by inactivation of notch signaling. *Curr Cancer Drug Targets* 2014; 14: 274-285.
- [86] Kang Q, Song WX, Luo Q, Tang N, Luo J, Luo X, Chen J, Bi Y, He BC, Park JK, Jiang W, Tang Y, Huang J, Su Y, Zhu GH, He Y, Yin H, Hu Z, Wang Y, Chen L, Zuo GW, Pan X, Shen J, Vokes T, Reid RR, Haydon RC, Luu HH and He TC. A comprehensive analysis of the dual roles of BMPs in regulating adipogenic and osteogenic differentiation of mesenchymal progenitor cells. *Stem Cells Dev* 2009; 18: 545-559.
- [87] Lu S, Wang J, Ye J, Zou Y, Zhu Y, Wei Q, Wang X, Tang S, Liu H, Fan J, Zhang F, Farina EM, Mohammed MM, Song D, Liao J, Huang J, Guo D,

Autophagy participates in BMP9-induced osteogenesis

- Lu M, Liu F, Liu J, Li L, Ma C, Hu X, Lee MJ, Reid RR, Ameer GA, Zhou D and He T. Bone morphogenetic protein 9 (BMP9) induces effective bone formation from reversibly immortalized multipotent adipose-derived (iMAD) mesenchymal stem cells. *Am J Transl Res* 2016; 8: 3710-3730.
- [88] Shu Y, Yang C, Ji X, Zhang L, Bi Y, Yang K, Gong M, Liu X, Guo Q, Su Y, Qu X, Nan G, Zhao C, Zeng Z, Yu X, Zhang R, Yan S, Lei J, Wu K, Wu Y, An L, Huang S, Gong C, Yuan C, Liu W, Huang B, Feng Y, Zhang B, Dai Z, Shen Y, Luo W, Wang X, Haydon RC, Luu HH, Reid RR, Wolf JM, Lee MJ, He TC and Li Y. Reversibly immortalized human umbilical cord-derived mesenchymal stem cells (UC-MSCs) are responsive to BMP9-induced osteogenic and adipogenic differentiation. *J Cell Biochem* 2018; 119: 8872-8886.
- [89] Zhao C, Qazvini NT, Sadati M, Zeng Z, Huang S, De La Lastra AL, Zhang L, Feng Y, Liu W, Huang B, Zhang B, Dai Z, Shen Y, Wang X, Luo W, Liu B, Lei Y, Ye Z, Zhao L, Cao D, Yang L, Chen X, Athiviraham A, Lee MJ, Wolf JM, Reid RR, Tirrell M, Huang W, de Pablo JJ and He TC. A pH-triggered, self-assembled, and bioprintable hybrid hydrogel scaffold for mesenchymal stem cell based bone tissue engineering. *ACS Appl Mater Interfaces* 2019; 11: 8749-8762.
- [90] Bi Y, He Y, Huang J, Su Y, Zhu GH, Wang Y, Qiao M, Zhang BQ, Zhang H, Wang Z, Liu W, Cui J, Kang Q, Zhang Z, Deng Y, Li R, Zhang Q, Yang K, Luu HH, Haydon RC, He TC and Tang N. Functional characteristics of reversibly immortalized hepatic progenitor cells derived from mouse embryonic liver. *Cell Physiol Biochem* 2014; 34: 1318-1338.
- [91] Yang K, Chen J, Jiang W, Huang E, Cui J, Kim SH, Hu N, Liu H, Zhang W, Li R, Chen X, Kong Y, Zhang J, Wang J, Wang L, Shen J, Luu HH, Haydon RC, Lian X, Yang T and He TC. Conditional immortalization establishes a repertoire of mouse melanocyte progenitors with distinct melanogenic differentiation potential. *J Invest Dermatol* 2012; 132: 2479-2483.
- [92] Li M, Chen Y, Bi Y, Jiang W, Luo Q, He Y, Su Y, Liu X, Cui J, Zhang W, Li R, Kong Y, Zhang J, Wang J, Zhang H, Shui W, Wu N, Zhu J, Tian J, Yi QJ, Luu HH, Haydon RC, He TC and Zhu GH. Establishment and characterization of the reversibly immortalized mouse fetal heart progenitors. *Int J Med Sci* 2013; 10: 1035-1046.
- [93] Wang N, Zhang W, Cui J, Zhang H, Chen X, Li R, Wu N, Chen X, Wen S, Zhang J, Yin L, Deng F, Liao Z, Zhang Z, Zhang Q, Yan Z, Liu W, Ye J, Deng Y, Wang Z, Qiao M, Luu HH, Haydon RC, Shi LL, Liang H and He TC. The piggyBac transposon-mediated expression of SV40 T antigen efficiently immortalizes mouse embryonic fibroblasts (MEFs). *PLoS One* 2014; 9: e97316.
- [94] Wu X, Li Z, Zhang H, He F, Qiao M, Luo H, Zhang J, Zhang M, Mao Y, Wagstaff W, Zhang Y, Niu C, Zhao X, Wang H, Huang L, Shi D, Liu Q, Ni N, Fu K, Haydon RC, Reid RR, Luu HH, He TC, Wang Z, Liang H, Zhang BQ and Wang N. Modeling colorectal tumorigenesis using the organoids derived from conditionally immortalized mouse intestinal crypt cells (ciMICs). *Genes Dis* 2021.
- [95] Yu X, Chen L, Wu K, Yan S, Zhang R, Zhao C, Zeng Z, Shu Y, Huang S, Lei J, Ji X, Yuan C, Zhang L, Feng Y, Liu W, Huang B, Zhang B, Luo W, Wang X, Liu B, Haydon RC, Luu HH, He TC and Gan H. Establishment and functional characterization of the reversibly immortalized mouse glomerular podocytes (imPODs). *Genes Dis* 2018; 5: 137-149.
- [96] Ye J, Wang J, Zhu Y, Wei Q, Wang X, Yang J, Tang S, Liu H, Fan J, Zhang F, Farina EM, Mohammed MK, Zou Y, Song D, Liao J, Huang J, Guo D, Lu M, Liu F, Liu J, Li L, Ma C, Hu X, Haydon RC, Lee MJ, Reid RR, Ameer GA, Yang L and He TC. A thermoresponsive polydiolcitrate-gelatin scaffold and delivery system mediates effective bone formation from BMP9-transduced mesenchymal stem cells. *Biomed Mater* 2016; 11: 025021.
- [97] Chen L, Jiang W, Huang J, He BC, Zuo GW, Zhang W, Luo Q, Shi Q, Zhang BQ, Wagner ER, Luo J, Tang M, Wietholt C, Luo X, Bi Y, Su Y, Liu B, Kim SH, He CJ, Hu Y, Shen J, Rastegar F, Huang E, Gao Y, Gao JL, Zhou JZ, Reid RR, Luu HH, Haydon RC, He TC and Deng ZL. Insulin-like growth factor 2 (IGF-2) potentiates BMP9-induced osteogenic differentiation and bone formation. *J Bone Miner Res* 2010; 25: 2447-2459.
- [98] Huang X, Wang F, Zhao C, Yang S, Cheng Q, Tang Y, Zhang F, Zhang Y, Luo W, Wang C, Zhou P, Kim S, Zuo G, Hu N, Li R, He TC and Zhang H. Dentinogenesis and tooth-alveolar bone complex defects in BMP9/GDF2 knockout mice. *Stem Cells Dev* 2019; 28: 683-694.
- [99] Su Y, Wagner ER, Luo Q, Huang J, Chen L, He BC, Zuo GW, Shi Q, Zhang BQ, Zhu G, Bi Y, Luo J, Luo X, Kim SH, Shen J, Rastegar F, Huang E, Gao Y, Gao JL, Yang K, Wietholt C, Li M, Qin J, Haydon RC, He TC and Luu HH. Insulin-like growth factor binding protein 5 suppresses tumor growth and metastasis of human osteosarcoma. *Oncogene* 2011; 30: 3907-3917.
- [100] Yan Z, Yin L, Wang Z, Ye J, Zhang Z, Li R, Denduluri SK, Wang J, Wei Q, Zhao L, Lu S, Wang X, Tang S, Shi LL, Lee MJ, He TC and Deng ZL. A novel organ culture model of mouse intervertebral disc tissues. *Cells Tissues Organs* 2016; 201: 38-50.
- [101] Wang X, Wu X, Zhang Z, Ma C, Wu T, Tang S, Zeng Z, Huang S, Gong C, Yuan C, Zhang L, Feng Y, Huang B, Liu W, Zhang B, Shen Y, Luo

Autophagy participates in BMP9-induced osteogenesis

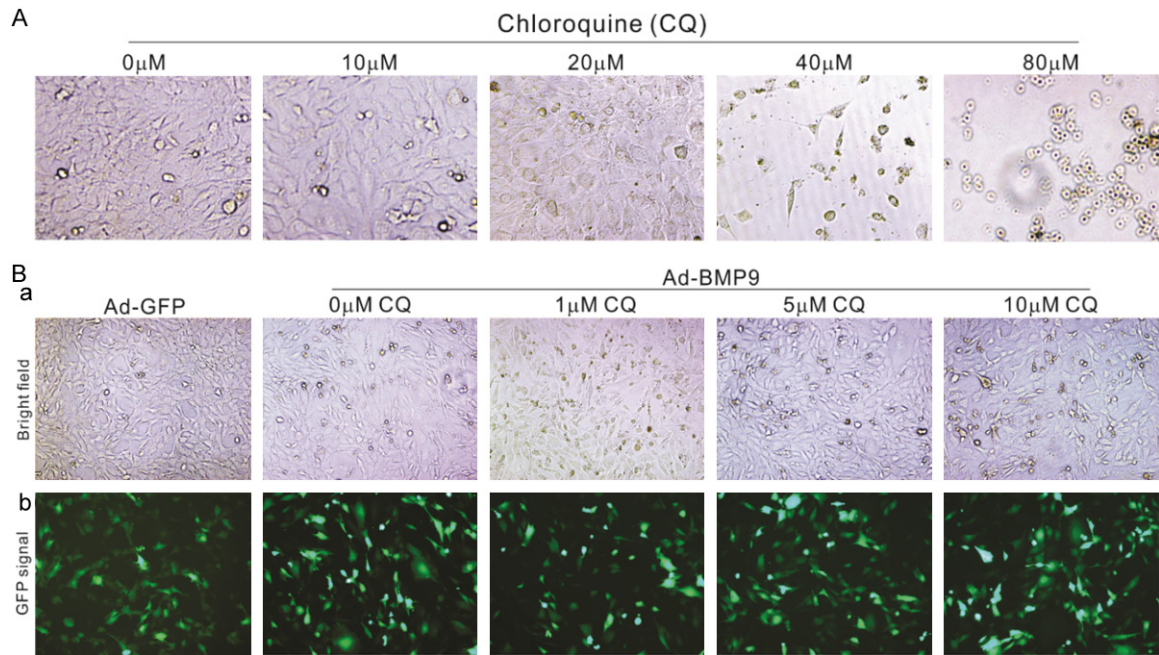
- W, Wang X, Liu B, Lei Y, Ye Z, Zhao L, Cao D, Yang L, Chen X, Haydon RC, Luu HH, Peng B, Liu X and He TC. Monensin inhibits cell proliferation and tumor growth of chemo-resistant pancreatic cancer cells by targeting the EGFR signaling pathway. *Sci Rep* 2018; 8: 17914.
- [102] Deng Y, Zhang J, Wang Z, Yan Z, Qiao M, Ye J, Wei Q, Wang J, Wang X, Zhao L, Lu S, Tang S, Mohammed MK, Liu H, Fan J, Zhang F, Zou Y, Liao J, Qi H, Haydon RC, Luu HH, He TC and Tang L. Antibiotic monensin synergizes with EGFR inhibitors and oxaliplatin to suppress the proliferation of human ovarian cancer cells. *Sci Rep* 2015; 5: 17523.
- [103] Yu X, Liu F, Zeng L, He F, Zhang R, Yan S, Zeng Z, Shu Y, Zhao C, Wu X, Lei J, Zhang W, Yang C, Wu K, Wu Y, An L, Huang S, Ji X, Gong C, Yuan C, Zhang L, Feng Y, Huang B, Liu W, Zhang B, Dai Z, Wang X, Liu B, Haydon RC, Luu HH, Gan H, He TC and Chen L. Niclosamide exhibits potent anticancer activity and synergizes with sorafenib in human renal cell cancer cells. *Cell Physiol Biochem* 2018; 47: 957-971.
- [104] Hu N, Jiang D, Huang E, Liu X, Li R, Liang X, Kim SH, Chen X, Gao JL, Zhang H, Zhang W, Kong YH, Zhang J, Wang J, Shui W, Luo X, Liu B, Cui J, Rogers MR, Shen J, Zhao C, Wang N, Wu N, Luu HH, Haydon RC, He TC and Huang W. BMP9-regulated angiogenic signaling plays an important role in the osteogenic differentiation of mesenchymal progenitor cells. *J Cell Sci* 2013; 126: 532-541.
- [105] Hu N, Wang C, Liang X, Yin L, Luo X, Liu B, Zhang H, Shui W, Nan G, Wang N, Wu N, Chen X, He Y, Wen S, Deng F, Zhang H, Liao Z, Luu HH, Haydon RC, He TC and Huang W. Inhibition of histone deacetylases potentiates BMP9-induced osteogenic signaling in mouse mesenchymal stem cells. *Cell Physiol Biochem* 2013; 32: 486-498.
- [106] Nuschke A, Rodrigues M, Stolz DB, Chu CT, Griffith L and Wells A. Human mesenchymal stem cells/multipotent stromal cells consume accumulated autophagosomes early in differentiation. *Stem Cell Res Ther* 2014; 5: 140.
- [107] Zahm AM, Bohensky J, Adams CS, Shapiro IM and Srinivas V. Bone cell autophagy is regulated by environmental factors. *Cells Tissues Organs* 2011; 194: 274-278.
- [108] Onal M, Piemontese M, Xiong J, Wang Y, Han L, Ye S, Komatsu M, Selig M, Weinstein RS, Zhao H, Jilka RL, Almeida M, Manolagas SC and O'Brien CA. Suppression of autophagy in osteocytes mimics skeletal aging. *J Biol Chem* 2013; 288: 17432-17440.
- [109] Piemontese M, Onal M, Xiong J, Han L, Thostenson JD, Almeida M and O'Brien CA. Low bone mass and changes in the osteocyte network in mice lacking autophagy in the osteoblast lineage. *Sci Rep* 2016; 6: 24262.
- [110] Piemontese M, Onal M, Xiong J, Wang Y, Almeida M, Thostenson JD, Weinstein RS, Manolagas SC and O'Brien CA. Suppression of autophagy in osteocytes does not modify the adverse effects of glucocorticoids on cortical bone. *Bone* 2015; 75: 18-26.
- [111] DeSelm CJ, Miller BC, Zou W, Beatty WL, van Meel E, Takahata Y, Klumperman J, Tooze SA, Teitelbaum SL and Virgin HW. Autophagy proteins regulate the secretory component of osteoclastic bone resorption. *Dev Cell* 2011; 21: 966-974.
- [112] Kang X, Yang W, Feng D, Jin X, Ma Z, Qian Z, Xie T, Li H, Liu J, Wang R, Li F, Li D, Sun H and Wu S. Cartilage-specific autophagy deficiency promotes ER stress and impairs chondrogenesis in PERK-ATF4-CHOP-dependent manner. *J Bone Miner Res* 2017; 32: 2128-2141.

Autophagy participates in BMP9-induced osteogenesis

Supplementary Table 1. List of oligonucleotides used in the study

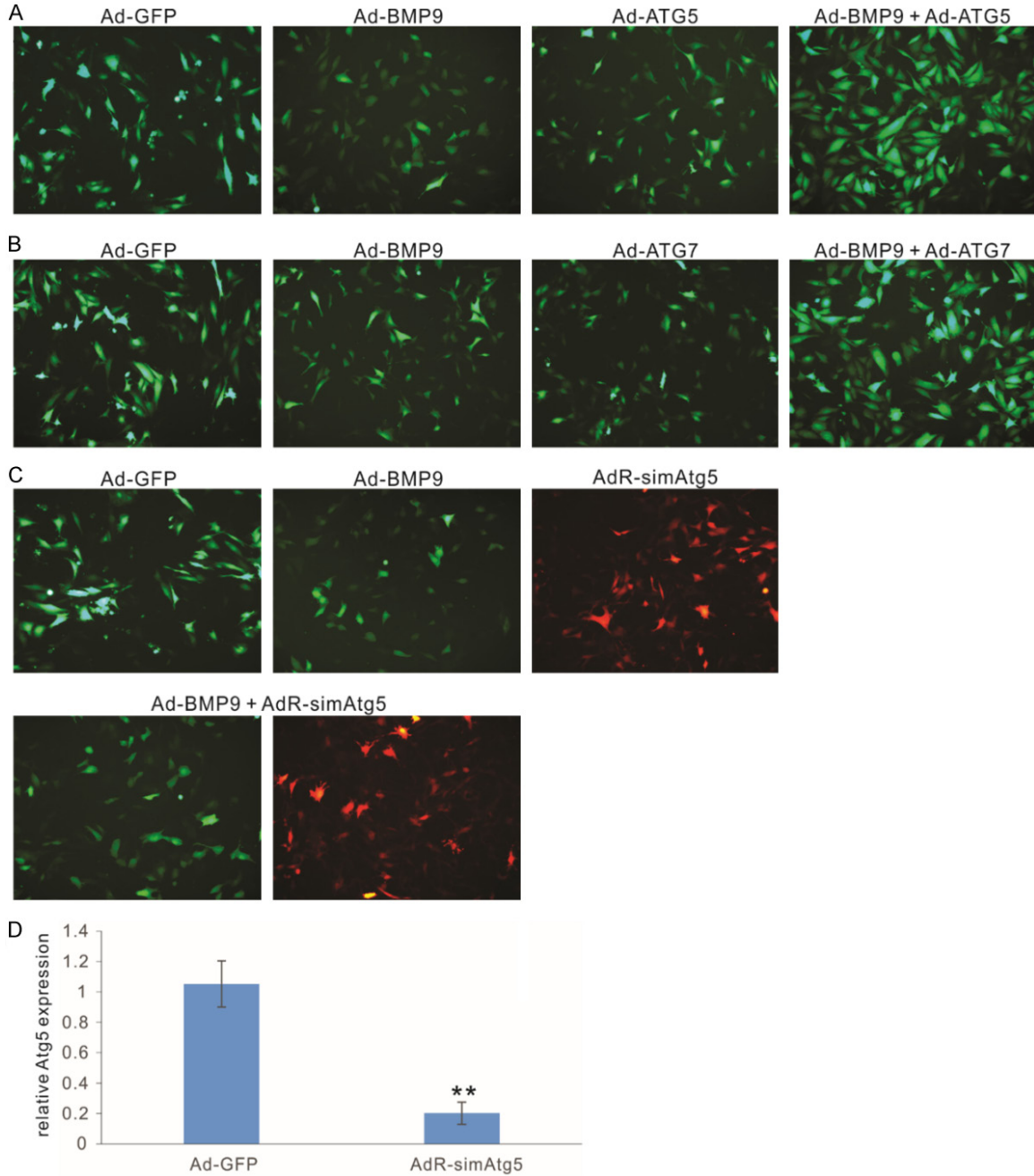
Gene	Sequence	Accession No.	Use
<i>Ulk1</i>	TGGTGTCACTGCAGAGCG CCGTGAGAGTGTGCTGCA	NM_009469.3	qPCR
<i>Fip200</i>	AGGACCGAGCTCGTTTGC TAGAGCTCTGGGGCTGCA	NM_009826	
<i>Atg3</i>	GCCCTATCGCTGCTCCAG CCCCTGTAGCCATTGCC	NM_026402.3	
<i>Atg5</i>	GGACAACGAGGCGTGACA GAGGCTGCAGTGGTCCTG	NM_053069.6	
<i>Atg6</i>	GTGGGGAAAGGACACCGG CTCCACGTCGCACACAGT	NM_019584	
<i>Atg7</i>	CGGCAGTTTCCAGTCCGT ATCCTCGGACCCATGCCT	NM_028835.4	
<i>Atg8</i>	CGCCGGAGTCAGATCGTC ATCTTGGTGGGGTGTGCTGC	NM_026160.5	
<i>Atg9a</i>	CGCTGGCTCTATCCTGGC CGGGGCAGAACACCATGT	NM_026160.5	
<i>Atg9b</i>	TGCCCTCGACAAGAAG GTTGAGGGTGTGGTCGGG	NM_001002897.3	
<i>Atg10</i>	GCGATGGCTGGGAATGGA TCACTTCTGCCACCGCTG	NM_025770.3	
<i>Atg12</i>	TCCTCGGCTGCAGTTTCG GTTGCTCCACAGCCCAT	NM_026217.3	
<i>Atg14</i>	TACACTATCAGCGCCGCG TCGCCACAGAACTCGCTG	NM_172599.4	
<i>Atg101</i>	CAGGTGGTGATGGCCTGG CCAAGGCTACCACGTGCA	NM_026566.2	
<i>Runx2</i>	CCGGTCTCCTCCAGGAT GGGAACTGCTGTGGCTTC	NM_001146038	
<i>Opn</i>	CCTCCCGGTGAAAGTGAC CTGTGGCGCAAGGAGATT	NM_001204201.1	
<i>Gapdh</i>	ACCCAGAAGACTGTGGATGG CACATTGGGGGTAGGAACAC	NM_008084.3	
<i>ATG5</i>	accaccatgggcATGACAGATGACAAAGATGTGCTTC TCAATCTGTTGGCTGTGGGATGATAC	NM_004849.3	over expression
<i>ATG7</i>	accaccATGGCGGCAGCTACGGGGGATCCTGG TCAGATGGTCTCATCATCGCTCATG	NM_001136031.2	
<i>Atg5</i>	aaaaaGCTTCGAGATGTGTGGTTTttttAGAGTGGTCT GgtGGTCTCGggcaaaaaGCTTCGAGATGTGTGGTTT aaaaaTAAAGTGAGCCTCAACCGCttttTTCGTCTTTT ggtGGTCTCGcgttAaaaaTAAAGTGAGCCTCAACCGC aaaaaATGAGTTTCCGGTTGATGGttttTTCGTCTTT ggtGGTCTCGgcaaaaaATGAGTTTCCGGTTGATGG	NM_053069	siRNAs

Autophagy participates in BMP9-induced osteogenesis



Supplementary Figure 1. Determination of sub-lethal and optimal concentrations of chloroquine (CQ) in MSCs. (A) Subconfluent MSCs were treated with the indicated concentrations of CQ and photographed at 72 h after treatment. Representative images are shown. (B) Subconfluent MSCs were infected with Ad-GFP or Ad-BMP9 and treated with CQ at the indicated concentrations. Bright field images (a) and GFP signal (b) were recorded at 48 h post infection/treatment. Representative images are shown.

Autophagy participates in BMP9-induced osteogenesis



Supplementary Figure 2. Characterization of the recombinant adenoviral vectors used in the study. (A, B) Efficient co-transduction of MSCs using BMP and Ad-ATG5 or Ad-ATG7 viral vectors. Subconfluent MSCs were infected with Ad-GFP, Ad-BMP9 and/or Ad-ATG5 (A) or Ad-ATG7 (B), and GFP signal was recorded at 48 h after infection. Representative images are shown. (C) Co-infection efficiency of AdR-simAtg5. Subconfluent MSCs were infected with Ad-GFP, Ad-BMP9 and/or AdR-simAtg5, and GFP or RFP signal was recorded at 48 h after infection. Representative images are shown. (D) Silencing efficiency of AdR-simAtg5. Subconfluent MSCs were infected with Ad-GFP, or AdR-simAtg5. At 72 h after infection, total RNA was isolated and subjected to RT-PCR analysis of Atg5 expression. “***” $P < 0.01$, compared with that of the Ad-GFP control group.